DREAM2S: Deformable Regions Driven by an Eulerian Accurate Minimization Method for Image and Video Segmentation

Stéphanie Jehan-Besson, Michel Barlaud, Gilles Aubert

International Journal of Computer Vision 53(1), 45–70, 2003

DREAM^{2}S: Deformable Regions Driven by an Eulerian Accurate Minimization Method for Image and Video Segmentation

STÉPHANIE JEHAN-BESSON AND MICHEL BARLAUD
Laboratoire I3S, CNRS-UNSA, 2000, route des Lucioles, 06903 Sophia Antipolis, France
jehan@i3s.unice.fr
barlaud@i3s.unice.fr

GILLES AUBERT
Laboratoire J.A. Dieudonné, CNRS-UNSA, Parc Valrose, 06108 Nice Cedex 2, France
gaubert@math.unice.fr

Received December 5, 2001; Revised December 10, 2002; Accepted December 12, 2002

Abstract. This paper deals with image and video segmentation using active contours. We propose a general form for the energy functional related to region-based active contours. We compute the associated evolution equation using shape derivation tools and accounting for the evolving region-based terms. Then we apply this general framework to compute the evolution equation from functionals that include various statistical measures of homogeneity for the region to be segmented. Experimental results show that the determinant of the covariance matrix appears to be a very relevant tool for segmentation of homogeneous color regions. As an example, it has been successfully applied to face segmentation in real video sequences.

Keywords: image segmentation, region segmentation, energy minimization, region-based active contours, region functionals, boundary functionals, shape optimization, shape gradient, partial differential equations, face segmentation, covariance matrix determinant, level sets

1. Introduction

Active contours are powerful tools for image and video segmentation. Since the original work on snakes (Kass et al., 1988), an extensive research has been performed that leads today to the use of "region-based active contours."

Originally, active contours were boundary-based methods (Aubert and Kornprobst, 2001). Snakes (Kass et al., 1988), balloons (Cohen, 1991) or geodesic active contours (Caselles et al., 1997) are driven towards the edges of an image. The evolution equation is computed from a criterion that only includes a local information on the boundary of the object to segment.

The key idea of region-based active contours, firstly proposed by Cohen et al. (1993) and Ronfard (1994), is to introduce a global information on the different regions to segment in addition to the boundary-based information, to make the active contour evolve. However, it is not trivial to compute the evolution equation of the active contour that will make it evolve towards a minimum of a criterion including both region-based and boundary-based terms.

Recently, many papers have addressed this problem. A review of these methods is proposed in Section 2. Some of these works do not compute the theoretical expression of the velocity vector of the active contour but they choose the displacement that will make the criterion decrease (Chakraborty et al., 1996; Chesnaud et al., 1999). Other works propose the computation of the velocity vector by reducing the whole problem to boundary integrals (Zhu and Yuille, 1996a; Paragios and Deriche, 1999a) or by using the level set method (Samson et al., 2000; Chan and Vese, 2001). They then use the Euler-Lagrange equations to compute the evolution equation.

The information on the different regions, that we call here "descriptor" of the corresponding region, may be globally attached to the region. Indeed it occurs for statistical descriptors such as the mean, the variance or the histogram of the region. In case of unsupervised segmentation, these descriptors are re-evaluated each time the active contour evolves and so they vary during the propagation of the active contour. Previous works on region-based active contours do not focus on this possible variation of the descriptors.

We propose here a general Eulerian framework for region-based active contours named DREAM^{2}S (Deformable Regions driven by an Eulerian Accurate Minimization Method for Segmentation). The main contribution of our work is to build a theoretical framework based on shape optimization principles. Indeed, shape optimization tools are well adapted for the derivation of region functionals. Besides, with such an approach, we can readily take into account the variation of the descriptors that are globally attached to the evolving regions (called region-dependent descriptors). We show that the variation of region-dependent descriptors during the evolution of the active contour induces additional terms in the evolution equation of the active contour.

Some examples of unsupervised spatial segmentation, using the variance of the regions, prove the importance of the additional terms for the accuracy of segmentation results. Finally, the determinant of the covariance matrix appears to be a very relevant tool for homogeneous color regions segmentation. This tool is successfully applied to face segmentation on real video sequences.

The detailed overview on region-based approaches is proposed in Section 2, while our Eulerian framework DREAM^{2}S is described in Section 3. This framework is then applied to unsupervised segmentation of homogeneous regions using the variance in Section 5 and the determinant of the covariance matrix in Section 6.

2. Problem Statement and State of the Art on Region-Based Active Contours

Recently, many authors have introduced region-based terms in the evolution equation driving active contours for segmentation issues. The problem statement is first presented and then the state-of-the-art is detailed.

2.1. Problem Statement

Here, we describe the equations addressing the issue of the segmentation of an image I in two regions. Let us define Ω_{in} the region containing the objects to segment and Ω_{out} the background region. Their common boundary is denoted by Γ. Let us consider an active contour $\Gamma(s,\tau) = (x(s,\tau), y(s,\tau))$, where s may be the arc length of the contour and τ is an evolution parameter. The active contour approach makes $\Gamma(s,\tau)$ evolve through the following partial differential equation (PDE) (Caselles et al., 1997; Malladi et al., 1995):

$$\frac{\partial \Gamma(s,\tau)}{\partial \tau} = F\boldsymbol{N} = \boldsymbol{v} \quad \text{with} \quad \Gamma(\tau = 0) = \Gamma_0$$

where Γ_0 is an initial curve defined by the user and $\boldsymbol{N}$ the inward normal vector of $\Gamma(s,\tau)$. The velocity F is derived from a minimizing criterion and is chosen so that the solution $\Gamma(.,\tau)$ converges to the object boundary, $\Gamma(.)$, as $\tau \to \infty$.

In classical boundary-based methods (Caselles et al., 1997), the velocity function F is derived from an energy J depending on the boundary Γ:

$$J_{boundary}(\Gamma) = \int_\Gamma k^{(b)}\, ds$$

where $k^{(b)}$ is a function describing the boundary of the object. Caselles et al. (1997) choose the function $k^{(b)} = g(|\nabla I|)$ where $g : [0, +\infty[\to \mathbb{R}^+$ is a strictly decreasing function so that $g(r) \to 0$ as $r \to \infty$. The computation of the velocity F from the criterion is now well known (Caselles et al., 1997) and leads to the following evolution equation:

$$\frac{\partial \Gamma}{\partial \tau} = \left[k^{(b)} \cdot \kappa - \nabla k^{(b)} \cdot \boldsymbol{N}\right]\boldsymbol{N}$$

where κ is the curvature of $\Gamma(\tau)$.

However, both regions Ω_{in} and Ω_{out} may have different properties of texture, homogeneity or motion that cannot be included in the function $k^{(b)}$. So the main purpose of region-based approaches is to introduce such a global information in the velocity function F in addition to the local information provided by boundary-based terms. The main question, in order to justify the introduction of these region terms, is to derive the velocity function from an energy. To set a general framework and to compare the different approaches proposed in the literature, we now introduce a general criterion from which the velocity magnitude may be derived:

$$\begin{aligned} J(\Omega_{in}, \Omega_{out}, \Gamma) = & \int\int_{\Omega_{out}} k^{(out)}(x, y, \Omega_{out})\, dx\, dy \\ & + \int\int_{\Omega_{in}} k^{(in)}(x, y, \Omega_{in})\, dx\, dy \\ & + \int_{\Gamma} k^{(b)}(x, y)\, ds \end{aligned} \tag{1}$$

where $k^{(out)}$ is named the "descriptor" of the background region, $k^{(in)}$ the "descriptor" of the object region and $k^{(b)}$ the "descriptor" of the contour. The region descriptors may be globally attached to their respective regions, Ω_{in} or Ω_{out}, and so depend on them (if so, they are called "region-dependent descriptors"). It happens when statistical features of a region like, for example, the mean or the variance, are selected as region descriptors.

The purpose of all region-based active contours methods is then to make the active contour evolve towards a partition of the image, $(\Omega_{out}, \Omega_{in}, \Gamma)$, that minimizes the criterion (1).

2.2. *Overview of Existing Region-Based Methods Using Active Contours*

While analysing region-based active contours approaches, we may consider two main important points:

- How is derived the evolution equation from the criterion?
- What are the different descriptors used?

Pioneer works have been proposed by Cohen et al. (1993) and Ronfard (1994). In an early work, Cohen et al. (1993) present a surface reconstruction method using region-based active contours. They compute the velocity vector of an active contour from the minimization of a criterion including region-based terms. In a pioneer work (Ronfard, 1994) assesses that the velocity function should be proportional to the difference of statistical features: $F = k^{(in)} - k^{(out)}$, where $k^{(in)}$ is a statistical model of the object region and $k^{(out)}$ a statistical model of the background region.

Some approaches propose to compute the evolution equation of the active contour using the Green-Riemann theorem and Euler-Lagrange equations. Zhu et al. (1995) and Zhu and Yuille (1996b) present a statistical framework for image segmentation using an algorithm called "region competition". They derive the active contour evolution equation by minimizing a generalized Bayes/MDL criterion inspired by the Mumford and Shah energy (1989). They propose the following descriptors for the segmentation of still images:

$$\begin{cases} k^{(out)} = -\log P(I(x, y)/\alpha_{out}) \\ k^{(in)} = -\log P(I(x, y)/\alpha_{in}) \\ k^{(b)} = \mu \end{cases}$$

where $P(\,)$ is a probability density function, α_i are the parameters of the distribution for the region i and μ is a positive constant (or linear model). For illustrations, the authors consider Gaussian distributions characterized by two parameters, the mean and the variance. Once the α_i fixed, the evolution equation of an active contour is computed and directly derived from the criterion. The classical derivative of the boundary-based term leads to the Euclidean geometric heat flow. The derivative of region-based terms is then performed using the Green-Riemann theorem and the Euler-Lagrange equations. Indeed, the computation of the evolution equation is performed in three main steps:

1. Transformation of domain integrals into boundary integrals using the Green-Riemann theorem.
2. Computation of the Euler-Lagrange equations
3. Introduction of a dynamical scheme in the Euler-Lagrange equations in order to compute the velocity vector of the active contour.

The velocity function F is then computed and it leads to the following evolution equation:

$$\frac{\partial \Gamma}{\partial \tau} = (k^{(in)} - k^{(out)} - \mu\kappa)\boldsymbol{N} \tag{2}$$

where κ is the curvature of $\Gamma(\tau)$. In order to implement this PDE, a Lagrangian formulation is used.

Recently, Paragios and Deriche (1999b, 2000, 2002a, 2002b), have proposed an extension of the work of Zhu and Yuille by improving the descriptor of the contour in order to incorporate the image gradient as in geodesic active contours. The evolution equation is implemented using the level set method introduced by Osher and Sethian (1988), Malladi et al. (1995) and Sethian (1996). A very interesting part of this work concerns the introduction of some descriptors $k^{(in)}$ and $k^{(out)}$ for applications like texture segmentation (Paragios and Deriche, 2002b) and moving objects detection (Paragios and Deriche, 1999b; Paragios and Deriche, 2002a).

Some other approaches (Chakraborty et al., 1996; Chesnaud et al., 1999) propose to choose at each step the displacement of the active contour that makes the criterion decrease. Chakraborty et al. (1996) introduce a region-based approach for the segmentation of medical images. As input of their algorithm, they consider both the actual image I and the region-classified image I_r. The classified image I_r is computed by maximizing the posterior distribution of the region labels given the intensity image. Their region term enforces the boundary to enclose a single region in I_r. The descriptors are the following with the difference that they want to maximize the criterion J:

$$\begin{cases} k^{(out)} = K_1 I_r(x, y) \\ k^{(in)} = 0 \\ k^{(b)} = K_2 I_g(x, y) \end{cases} \tag{3}$$

where K_1 and K_2 are two positive constants and I_g is the gradient image. A prior shape term is also added to the criterion, which can be interesting for medical imaging where the nature of the shape does not change a lot from individual to individual. Then, as in Zhu and Yuille (1996a), the whole problem is reduced to computing boundary integrals thanks to the Green-Riemann theorem, rather than both boundary and domain integrals. The implementation of the active contour in Chakraborty et al. (1996) is done by using a Fourier parameterization. The expression of the velocity vector of the active contour is not computed, but the criterion is introduced and numerically evaluated in order to maximize it. We can note that the authors have proposed a very interesting extension of this work using the game theory (Chakraborty and Duncan, 1999). Region and boundary criterions are separated, but each criterion contains an interaction with the other. As the game progresses, both modules improve their positions through mutual information sharing.

Another similar approach has been introduced by Chesnaud et al. (1999). Their descriptors are re-evaluated each time a point of the active contour evolves since their descriptors are statistical features of the image globally attached to the evolving regions. They choose the random displacement of a considered point of the active contour so that the criterion decreases. After each displacement of a point of the active contour, the descriptors are re-computed.

A later approach has been introduced by Samson et al. (2000) for classification and by Chan and Vese (2001) for segmentation of still images. They propose to embed the criterion directly in the level set formulation. Chan and Vese propose the following descriptors:

$$\begin{cases} k^{(out)} = \lambda_1 |I - c_1|^2 + \nu \\ k^{(in)} = \lambda_2 |I - c_2|^2 \\ k^{(b)} = \mu \end{cases}$$

with c_1 the average of I in Ω_{in}, c_2 the average of I in Ω_{out}. These two values are re-estimated during the propagation of the curve as the regions evolve. The parameters λ_1, λ_2, ν and μ are some positive constants. Here the level set method is directly used by representing the curve $\Gamma(\tau)$ as the zero level set of a Lipschitz continuous function $U(x, y, \tau)$. The level set function U is introduced in the criterion via the Heaviside function $H(U)$. The criterion is then minimized with respect to U using a regularized version of the minimization problem. The evolution equation is directly expressed with the level set function and not with the curve Γ.

Some other works, have been proposed by Debreuve et al. (2001) for medical imaging and by Amadieu et al. (1999) for building detection.

Finally, region-based active contours are also powerful tools for classification (Yezzi et al., 1999) or motion detection (Mansouri and Konrad, 1999).

The major contribution of our work is to propose a general framework for region-based active contours. The velocity vector of the active contour is computed by introducing a dynamical scheme directly in the criterion to minimize as in Debreuve et al. (2001) and Amadieu et al. (1999). However, we propose here a new formulation of the derivation using shape optimization tools. To our knowledge, shape optimization tools have been used only for the computation of the optical flow (Schnörr, 1992). Besides, we focus on the case of region-dependent descriptors that vary during the propagation of the active contour. For such region-dependent descriptors, we show that additional terms appear in the evolution equation of the curve that have not been previously computed.

3. Setting a General Framework for Region-Based Active Contours

Our main goal lies in the elaboration of a general framework for the segmentation of an image in two different regions using region-based active contours.

We propose to minimize the general criterion (1) where each region is described using a function called "descriptor of the region". As previously detailed, a descriptor is a function that measures the homogeneity of a region. Most of relevant statistical descriptors depend themselves on the region. Some examples are given in Section 3.5. For example, the region descriptor $k^{(in)}$ can be chosen as the variance σ_{in}^2 of the region Ω_{in}, which gives:

$$k^{(in)}(x, y, \Omega_{in}) = \sigma_{in}^2 = \frac{\int\int_{\Omega_{in}} (I - \mu_{in})^2 \, dx \, dy}{\int\int_{\Omega_{in}} dx \, dy}$$

where μ_{in} is the mean of the region Ω_{in}. Such a descriptor is named a "region-dependent descriptor" since it depends on the region Ω_{in}.

Once the criterion is introduced, we propose to compute the evolution equation of the contour that will make it evolve towards a minimum of the criterion using a new Eulerian method. It fundamentally differs from other approaches since we keep the formulation of regions instead of reducing the whole problem to boundary integrals. Indeed, we first introduce a dynamical scheme in the criterion and then we compute the Eulerian derivative of the evolving criterion by using shape optimization computation.

The computation of the evolution equation of the active contour is performed in three main steps:

1. *Introduction of a dynamical scheme*: We search for the partition of the image $(\Omega_{in}, \Omega_{out}, \Gamma)$ which minimizes the criterion $J(\Omega_{in}, \Omega_{out}, \Gamma)$ described in (1). While assuming that an optimal partition exists, the issue is to compute this solution. However, it is difficult to compute the derivative of the criterion according to the domains. To circumvent this problem, we apply a transformation T_τ to the initial domain, such that it becomes continuously dependent on an evolution parameter τ. The criterion becomes dependent on τ: $J(\tau) = J(\Omega_{in}(\tau), \Omega_{out}(\tau), \Gamma(\tau))$. In this dynamical scheme, we can readily take into account a possible variation of the descriptors with the evolving regions $T_\tau(\Omega_i(0)) = \Omega_i(\tau)$.
2. *Derivation of the criterion using shape optimization theorems*: Thanks to the chain rule and by using shape optimization results, we compute the derivative of $J(\tau)$ with respect to τ, which is new in the area of active contours. The variation of the descriptors with the evolving regions $\Omega_i(\tau)$ (and so with τ) is taken into account.
3. *Computation of the evolution equation from the derivative*: From the derivative, we deduce the velocity vector of the active contour that will make it evolve as fast as possible towards a minimum of the criterion.

This general framework can be applied to many different applications by only changing the descriptors. It has been first applied to moving objects detection in video sequences acquired either with a static (Jehan-Besson et al., 2001b; Jehan-Besson et al., 2000) or a mobile camera (Jehan-Besson et al., 2001a). Descriptors may also be sequentially used to improve the final result as it has been proposed in Jehan-Besson et al. (2002). The method was recently applied to image segmentation using histograms (Aubert et al., to appear).

3.1. *Introduction of a Dynamical Scheme*

An image $I(x, y)$ is a function defined for $(x, y) \in \Omega \subset \mathbb{R}^2$, where Ω is the image domain. The image domain is considered to be made up of two parts (Fig. 1): the foreground part containing the objects to segment, denoted by Ω_{in}, and the background part denoted by Ω_{out}. The discontinuity set is a curve noted Γ that defines the boundary between the two domains.

We then search for the two domains Ω_{out} and Ω_{in} which minimize the criterion J reminded

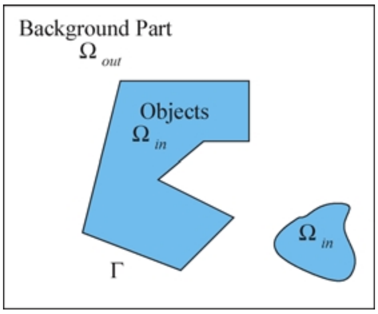

Figure 1. The two regions of an image.

here:

$$J(\Omega_{out}, \Omega_{in}, \Gamma) = \int\int_{\Omega_{out}} k^{(out)}(x, y, \Omega_{out})\, dx\, dy + \int\int_{\Omega_{in}} k^{(in)}(x, y, \Omega_{in})\, dx\, dy + \int_{\Gamma(\tau)} k^{(b)}(x, y)\, ds$$

In criterion (1), the first two terms are region-based while the third term is boundary-based. The functions $k^{(out)}$, $k^{(in)}$ and $k^{(b)}$ are respectively the descriptors of the background part, of the objects to segment and of the contour. The descriptors may be globally attached to the evolving regions and so depend on Ω_{in} or Ω_{out}.

We cannot compute the derivative of the previous criterion according to domains. Therefore, to compute an optimal solution, a dynamical scheme is introduced where each domain becomes continuously dependent on an evolution parameter τ. To formalize this idea, we may suppose that the evolution process is totally determined by the existence of a family of mappings T_τ that transforms the initial domains $\Omega_{in}(0)$ and $\Omega_{out}(0)$ into the current domains $\Omega_{in}(\tau)$ and $\Omega_{out}(\tau)$:

$$\begin{array}{l} \Omega_i(0) \xrightarrow{T_\tau} \Omega_i(\tau) \\ \Gamma(0) \xrightarrow{T_\tau} \Gamma(\tau) \end{array} \quad \text{where } i = in \text{ or } out.$$

The role of the triplet $\{\Omega_{out}(\tau), \Omega_{in}(\tau), \Gamma(\tau)\}$ is to formally act as a minimizing sequence for $J(\Omega_{out}, \Omega_{in}, \Gamma)$ when τ evolves. In fact we want that the functional $J(\Omega_{out}(\tau), \Omega_{in}(\tau), \Gamma(\tau))$ decreases as τ increases. The criterion then becomes:

$$J(\Omega_{out}(\tau), \Omega_{in}(\tau), \Gamma(\tau)) = \int\int_{\Omega_{out}(\tau)} k^{(out)}(x, y, \Omega_{out}(\tau))\, dx\, dy + \int\int_{\Omega_{in}(\tau)} k^{(in)}(x, y, \Omega_{in}(\tau))\, dx\, dy + \int_{\Gamma(\tau)} k^{(b)}(x, y)\, ds$$

The functional $J(\Omega_{out}(\tau), \Omega_{in}(\tau), \Gamma(\tau))$ is thereafter denoted by $J(\tau)$, and the descriptors $k^{(in)}(x, y, \Omega_{in}(\tau))$ and $k^{(out)}(x, y, \Omega_{out}(\tau))$ are respectively denoted by $k^{(in)}(x, y, \tau)$ and $k^{(out)}(x, y, \tau)$, which leads to the following expression:

$$J(\tau) = \int\int_{\Omega_{out}(\tau)} k^{(out)}(x, y, \tau)\, dx\, dy + \int\int_{\Omega_{in}(\tau)} k^{(in)}(x, y, \tau)\, dx\, dy + \int_{\Gamma(\tau)} k^{(b)}(x, y)\, ds$$

Hence we consider that $\Gamma(\tau)$ is modelled as an active contour that converges towards the final expected segmentation.

Let $\Gamma(0)$ be the initial curve defined by the user. We recall that we search for $\Gamma(\tau)$ as a curve evolving according to the following PDE:

$$\frac{\partial \Gamma(s, \tau)}{\partial \tau} = \boldsymbol{v} \quad \text{with} \quad \Gamma(0) = \Gamma_0$$

where $\boldsymbol{v}$ is the velocity vector of the active contour. The main problem lies in finding the velocity $\boldsymbol{v}$ from the criterion in order to get the fastest curve evolution towards the final segmentation.

3.2. *Computation of the Derivative of the Criterion*

In order to obtain the evolution equation, the criterion $J(\tau)$ must be differentiated with respect to τ. The integral bounds depend on τ and the descriptors $k^{(out)}(\,)$ and $k^{(in)}(\,)$ may also depend on τ.

Let us define the functional $k(x, y, \tau)$ such that:

$$k(x, y, \tau) = \begin{cases} k^{(out)}(x, y, \tau) & \text{if } (x, y) \in \Omega_{out}(\tau) \\ k^{(in)}(x, y, \tau) & \text{if } (x, y) \in \Omega_{in}(\tau) \end{cases} \tag{4}$$

The functional $k^{(out)}(\,)$ and $k^{(in)}(\,)$ are defined on the whole image domain Ω. Then, the criterion $J(\tau)$ writes as:

$$J(\tau) = \int_\Omega k(x, y, \tau)\,dx\,dy + \int_{\Gamma(\tau)} k^{(b)}(x, y)\,ds$$
$$= J_1(\tau) + J_2(\tau) \tag{5}$$

where Ω is the image domain, and:

$$J_1(\tau) = \int_\Omega k(x, y, \tau)\,dx\,dy$$
$$J_2(\tau) = \int_{\Gamma(\tau)} k^{(b)}(x, y)\,ds$$

In order to compute the derivative of the criterion $J_1(\tau)$, the discontinuities must explicitly be taken into account. For such a purpose, we first recall a general theorem concerning the derivative of a time-dependent criterion.

Let us define $\Omega(\tau)$ as a region included into Ω.

Theorem 1. *Let k be a smooth function on $\bar{\Omega} \times (0, T)$, and let $J(\tau) = \int\int_{\Omega(\tau)} k(x, y, \tau)\,dx\,dy$, then:*

$$\frac{dJ}{d\tau} = J'(\tau) = \int\int_{\Omega(\tau)} \frac{\partial k}{\partial \tau}\,dx\,dy - \int_{\partial\Omega(\tau)} k(\boldsymbol{v} \cdot \boldsymbol{N}_{\partial\Omega})\,ds$$

where $\boldsymbol{v}$ is the velocity of $\partial\Omega(\tau)$ and $\boldsymbol{N}_{\partial\Omega}$ is the unit inward normal to $\partial\Omega(\tau)$.

The derivative of J with respect to τ is the Eulerian derivative of $J(\Omega)$ in the direction of $\boldsymbol{V}$, whose proof can be found in Sokolowski and Zolésio (1992) and Delfour and Zolésio (2001). We provide in Appendix A, an elementary proof for completeness. The variation of J is due to the variation of the functional $k(x, y, \tau)$ and to the motion of the integral domain $\Omega(\tau)$.

As a corollary of Theorem 1, we get:

Corollary 1. *Let us suppose that the domain $\Omega(\tau)$ is made up of two parts, $\Omega_{in}(\tau)$ and $\Omega_{out}(\tau)$ separated by a moving interface $\Gamma(\tau)$ whose velocity is $\boldsymbol{v}$. The function $k(x, y, \tau)$ is supposed to be separately continuous in $\Omega_{in}(\tau)$ and $\Omega_{out}(\tau)$ but may be discontinuous across $\Gamma(\tau)$. We note $k^{(in)}$ and $k^{(out)}$, the value of k in respectively $\Omega_{in}(\tau)$ and $\Omega_{out}(\tau)$. Thus the derivative of $J(\tau)$ writes as:*

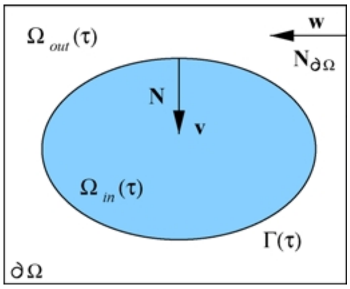

Figure 2. The domains and the vectors involved in the derivation.

$$J'(\tau) = \int\int_{\Omega(\tau)} \frac{\partial k}{\partial \tau}\,dx\,dy - \int_{\partial\Omega(\tau)} k(\boldsymbol{w} \cdot \boldsymbol{N}_{\partial\Omega})\,ds + \int_{\Gamma(\tau)} [[k]](\boldsymbol{v} \cdot \boldsymbol{N})\,ds$$

where $[[k]]$ represents the jump of k across $\Gamma(\tau)$: $[[k]] = k^{(out)} - k^{(in)}$, $\boldsymbol{N}$ the unit normal of $\Gamma(\tau)$ directed from $\Omega_{out}(\tau)$ to $\Omega_{in}(\tau)$, $\boldsymbol{N}_{\partial\Omega}$ the unit inward normal to $\partial\Omega(\tau)$ and $\boldsymbol{w}$ the velocity vector of $\partial\Omega(\tau)$.

Proof: We can apply Theorem 1 to the domain $\Omega_{in}(\tau)$ and to the domain $\Omega_{out}(\tau)$. Adding the two equations, we obtain the corollary. □

It is now straightforward to get the derivative of the criterion $J_1(\tau)$: we take $\Omega(\tau) = \Omega$ the image domain (Fig. 2). Then, by explicitly taking the discontinuities into account thanks to the Corollary, the derivative of $J_1(\tau)$ is given by:

$$J_1'(\tau) = \int_{\Gamma(\tau)} [[k]](\boldsymbol{v} \cdot \boldsymbol{N})\,ds - \int_{\partial\Omega} k(\boldsymbol{w} \cdot \boldsymbol{N}_{\partial\Omega})\,ds + \int\int_{\Omega_{in}(\tau)} \frac{\partial k^{(in)}}{\partial \tau}\,dx\,dy + \int\int_{\Omega_{out}(\tau)} \frac{\partial k^{(out)}}{\partial \tau}\,dx\,dy \tag{6}$$

Obviously, the second term of the derivative (6) is zero since the external boundary $\partial\Omega$ of the image is fixed.

Replacing $[[k]]$ with its expression, we find:

$$J_1'(\tau) = \int_{\Gamma(\tau)} \big(k^{(out)} - k^{(in)}\big)(\boldsymbol{v}\cdot\boldsymbol{N})\,ds + \int\int_{\Omega_{in}(\tau)} \frac{\partial k^{(in)}}{\partial\tau}\,dx\,dy + \int\int_{\Omega_{out}(\tau)} \frac{\partial k^{(out)}}{\partial\tau}\,dx\,dy \tag{7}$$

The derivative of $J_2(\tau)$ is classical:

$$J_2'(\tau) = \int_{\Gamma(\tau)} \big(-k^{(b)}\cdot\kappa + \nabla k^{(b)}\cdot\boldsymbol{N}\big)(\boldsymbol{v}\cdot\boldsymbol{N})\,ds$$

where $\kappa(x, y, \tau)$ is the curvature of $\Gamma(x, y, \tau)$. Therefore, the derivative of the whole criterion is the following:

$$J'(\tau) = \int\int_{\Omega_{in}(\tau)} \frac{\partial k^{(in)}}{\partial\tau}\,dx\,dy + \int\int_{\Omega_{out}(\tau)} \frac{\partial k^{(out)}}{\partial\tau}\,dx\,dy + \int_{\Gamma(\tau)} \big(k^{(out)} - k^{(in)} - k^{(b)}\cdot\kappa + \nabla k^{(b)}\cdot\boldsymbol{N}\big)(\boldsymbol{v}\cdot\boldsymbol{N})\,ds \tag{8}$$

3.3. *Expression of the Derivative According to the Unknown Velocity Vector* $\boldsymbol{v}$

3.3.1. Expression of the Descriptors. Here we take the general case where the descriptors depend on features globally attached to the region and so may depend on τ. We model each descriptor as a combination of features globally attached to the evolving regions $\Omega_{in}(\tau)$ or $\Omega_{out}(\tau)$:

$$\begin{aligned} k^{(in)}(x, y, \tau) &= g^{(in)}\big(x, y, G_1^{(in)}(\tau), G_2^{(in)}(\tau), \ldots, G_p^{(in)}(\tau)\big) \\ k^{(out)}(x, y, \tau) &= g^{(out)}\big(x, y, G_1^{(out)}(\tau), G_2^{(out)}(\tau), \ldots, G_m^{(out)}(\tau)\big) \end{aligned} \tag{9}$$

where:

$$G_j^{(\cdot)} = \int\int_{\Omega\cdot(\tau)} H_j^{(\cdot)}(x, y, \tau)\,dx\,dy \quad \text{with} \quad (\cdot) = (in) \text{ or } (out).$$

The functional $H_j^{(\cdot)}$ may also be region-dependent, more precisely we define:

$$\begin{aligned} H_j^{(in)}(x, y, \tau) &= H_j^{(in)}\big(x, y, K_{j1}^{(in)}(\tau), K_{j2}^{(in)}(\tau), \ldots, K_{jl_j}^{(in)}(\tau)\big) \\ H_j^{(out)}(x, y, \tau) &= H_j^{(out)}\big(x, y, K_{j1}^{(out)}(\tau), K_{j2}^{(out)}(\tau), \ldots, K_{jk_j}^{(out)}(\tau)\big) \end{aligned} \tag{10}$$

where:

$$K_{ji}^{(\cdot)}(\tau) = \int\int_{\Omega.(\tau)} L_{ji}^{(\cdot)}(x, y)\,dx\,dy$$

We stopped the process at the second level by choosing $L_{ji}^{(\cdot)}$ region-independent, but it could conceivably continue. The descriptors proposed in this paper fit to this framework. More complicated descriptors may also be studied easily with the method of derivation proposed. Let us first compute the derivative of $k^{(in)}$, we find:

$$\frac{\partial k^{(in)}}{\partial\tau} = \sum_{j=1}^{p} \frac{\partial g^{(in)}}{\partial G_j^{(in)}}\big(x, y, G_1^{(in)}(\tau), \ldots, G_p^{(in)}(\tau)\big)\frac{\partial G_j^{(in)}}{\partial\tau}(\tau)$$

We have now to compute the derivative of $G_j^{(in)}$ according to τ. We apply Theorem 1 and we get:

$$\frac{\partial G_j^{(in)}}{\partial\tau} = \int\int_{\Omega_{in}(\tau)} \frac{\partial H_j^{(in)}}{\partial\tau}\,dx\,dy - \int_{\Gamma(\tau)} H_j^{(in)}(\boldsymbol{v}\cdot\boldsymbol{N})\,ds$$

We may now compute the derivative of $H_j^{(in)}$ according to τ. Applying the chain rule, we get:

$$\frac{\partial H_j^{(in)}}{\partial\tau} = \sum_{i=1}^{l_j} \frac{\partial H_j^{(in)}}{\partial K_{ji}^{(in)}}\big(x, y, K_{j1}^{(in)}(\tau), \ldots, K_{jl_i}^{(in)}(\tau)\big)\frac{\partial K_{ji}^{(in)}}{\partial\tau}(\tau)$$

We compute the derivative of $K_{ji}^{(in)}$ according to τ. We apply Theorem 1 and we get:

$$\frac{\partial K_{ji}^{(in)}}{\partial\tau} = \int\int_{\Omega_{in}(\tau)} \frac{\partial L_{ji}^{(in)}}{\partial\tau}\,dx\,dy - \int_{\Gamma(\tau)} L_{ji}^{(in)}(\boldsymbol{v}\cdot\boldsymbol{N})\,ds \tag{11}$$

Since we stopped the process at the second level, we define L_{ji} as region-independent and so $\partial L_{ji}^{(in)}/\partial\tau = 0$ and the first term of Eq. (11) is nul. We can then compute the whole expression of the derivative of $G_j^{(in)}$:

$$\frac{\partial G_j^{(in)}}{\partial\tau} = -\sum_{i=1}^{lj} B_{ji}^{(in)} \int_{\Gamma(\tau)} L_{ji}^{(in)}(\boldsymbol{v}\cdot\boldsymbol{N})\,ds - \int_{\Gamma(\tau)} H_j^{(in)}(\boldsymbol{v}\cdot\boldsymbol{N})\,ds$$

where:

$$B_{ji}^{(in)} = \int\int_{\Omega_{in}(\tau)} \frac{\partial H_j^{(in)}}{\partial K_{ji}^{(in)}}\Big(x, y, K_{j1}^{(in)}(\tau), \ldots, K_{jl_i}^{(in)}(\tau)\Big)\,dx\,dy$$

Replacing the derivatives of $G_j^{(in)}$ by their expressions, we obtain the following expression for the derivative of the descriptor $k^{(in)}$:

$$\begin{aligned}\int\int_{\Omega_{in}(\tau)} \frac{\partial k^{(in)}}{\partial\tau}\,dx\,dy &= -\sum_{j=1}^{p} A_j^{(in)} \sum_{i=1}^{lj} B_{ji}^{(in)} \int_{\Gamma(\tau)} L_{ji}^{(in)}(\boldsymbol{v}\cdot\boldsymbol{N})\,ds \\ &\quad - \sum_{j=1}^{p} A_j^{(in)} \int_{\Gamma(\tau)} H_j^{(in)}(\boldsymbol{v}\cdot\boldsymbol{N})\,ds \end{aligned} \tag{12}$$

where:

$$A_j^{(in)} = \int\int_{\Omega_{in}(\tau)} \frac{\partial g^{(in)}}{\partial G_j^{(in)}}\Big(x, y, G_1^{(in)}(\tau), \ldots, G_p^{(in)}(\tau)\Big)\,dx\,dy$$

The expression for $(\cdot) = (out)$ is computed in the same manner while paying attention to the direction of the normal vector, and we thus obtain the general expression for the derivative of $J(\tau)$:

$$\begin{aligned} J'(\tau) &= \int_{\Gamma(\tau)} \Big(k^{(out)} - k^{(in)} - k^{(b)}\cdot\kappa + \nabla k^{(b)}\cdot\boldsymbol{N}\Big)(\boldsymbol{v}\cdot\boldsymbol{N})\,ds \\ &\quad - \sum_{j=1}^{p} A_j^{(in)} \int_{\Gamma(\tau)} H_j^{(in)}(\boldsymbol{v}\cdot\boldsymbol{N})\,ds \\ &\quad + \sum_{j=1}^{m} A_j^{(out)} \int_{\Gamma(\tau)} H_j^{(out)}(\boldsymbol{v}\cdot\boldsymbol{N})\,ds \\ &\quad - \sum_{j=1}^{p} A_j^{(in)} \sum_{i=1}^{lj} B_{ji}^{(in)} \int_{\Gamma(\tau)} L_{ji}^{(in)}(\boldsymbol{v}\cdot\boldsymbol{N})\,ds \\ &\quad + \sum_{j=1}^{m} A_j^{(out)} \sum_{i=1}^{kj} B_{ji}^{(out)} \int_{\Gamma(\tau)} L_{ji}^{(out)}(\boldsymbol{v}\cdot\boldsymbol{N})\,ds \end{aligned} \tag{13}$$

3.4. From the Derivative Towards the Evolution Equation of the Active Contour

The goal of this part is to compute the expression of the velocity vector $\boldsymbol{v}$ which makes the curve evolve as fast as possible towards a minimum of the criterion J. According to the Cauchy-Schwartz inequality, the fastest decrease of $J(\tau)$ is obtained from (13) by choosing $\boldsymbol{v} = F\boldsymbol{N}$ which leads to the following evolution equation:

$$\begin{aligned}\frac{\partial\Gamma(\tau)}{\partial\tau} = \Bigg[& k^{(in)} - k^{(out)} + k^{(b)}\cdot\kappa - \nabla k^{(b)}\cdot\boldsymbol{N} \\ & + \sum_{j=1}^{p} A_j^{(in)} H_j^{(in)} - \sum_{j=1}^{m} A_j^{(out)} H_j^{(out)} \\ & + \sum_{j=1}^{p} A_j^{(in)} \sum_{i=1}^{lj} B_{ji}^{(in)} L_{ji}^{(in)} \\ & - \sum_{j=1}^{m} A_j^{(out)} \sum_{i=1}^{kj} B_{ji}^{(out)} L_{ji}^{(out)} \Bigg]\boldsymbol{N} \end{aligned} \tag{14}$$

If the descriptors do not depend on τ (region-independent descriptors), the PDE reduces to the following expression:

$$\frac{\partial\Gamma(\tau)}{\partial\tau} = \big[k^{(in)} - k^{(out)} + k^{(b)}\cdot\kappa - \nabla k^{(b)}\cdot\boldsymbol{N}\big]\boldsymbol{N}$$

We can notice that the dependence of the descriptors on τ, and so on the curve evolution, induces additional terms in the evolution equation of the active contour. We can also remark that the velocity of the contour in (14) can be positive or negative. This an interesting property of region-based active contours. On the contrary to boundary-based active contours, region-based active contours allow some parts of the curve to shrink while others expand. Thus the initialization is less constrained.

3.5. *Computation of the Evolution Equation for Some Examples of Descriptors*

The goal of this part is to compute the evolution equation of the active contour for some examples of region-dependent descriptors. Let us take some descriptors depending on the mean μ_{in} or on the variance σ_{in} of the evolving region $\Omega_{in}(\tau)$:

$$\begin{cases} \mu_{in}(\tau) = \frac{1}{|\Omega_{in}|} \int\int_{\Omega_{in}(\tau)} I dx\, dy \quad \text{with} \\ |\Omega_{in}| = \int\int_{\Omega_{in}(\tau)} dx\, dy \\ \sigma_{in}^2(\tau) = \frac{1}{|\Omega_{in}|} \int\int_{\Omega_{in}(\tau)} (I - \mu_{in}(\tau))^2\, dx\, dy \end{cases}$$

3.5.1. Descriptors depending on the variance. We choose the following set of descriptors:

$$\begin{cases} k^{(out)} \text{ does not depend on } \tau \\ k^{(in)} = \varphi(\sigma_{in}^2) \end{cases}$$

where $\varphi(r)$ is a positive function of class C^1 ($\mathbb{R}$).

This velocity vector is computed by replacing the terms of (13) with their expressions. We first express the descriptor $k^{(in)}$ as a combination of domains integrals:

$$\begin{aligned} k^{(in)}(x, y, \tau) &= g^{(in)}\big(x, y, G_1^{(in)}(\tau), G_2^{(in)}(\tau)\big) \\ &= \varphi\left(\frac{G_1^{(in)}(\tau)}{G_2^{(in)}(\tau)}\right) \end{aligned}$$

where:

$$\begin{aligned} G_1^{(in)}(\tau) &= \int\int_{\Omega_{in}(\tau)} H_1^{(in)}(x, y, \tau)\, dx\, dy \\ G_2^{(in)}(\tau) &= \int\int_{\Omega_{in}(\tau)} H_2^{(in)}(x, y, \tau)\, dx\, dy \end{aligned}$$

with

$$\begin{aligned} H_1^{(in)}(x, y, \tau) &= (I(x, y) - \mu_{in}(\tau))^2 \\ H_2^{(in)}(x, y, \tau) &= 1 \end{aligned}$$

or:

$$\begin{aligned} &H_1^{(in)}(x, y, \tau) = \left(I(x, y) - \frac{K_{11}^{(in)}}{K_{12}^{(in)}}\right)^2, \quad l_1 = 2, \\ &H_2^{(in)}(x, y, \tau) = 1, \quad l_2 = 0, \end{aligned}$$

with:

$$\begin{aligned} K_{11}^{(in)}(x, y, \tau) &= \int\int_{\Omega_{in}(\tau)} I(x, y)\, dx\, dy, \\ L_{11}^{(in)}(x, y) &= I(x, y), \\ K_{12}^{(in)}(x, y, \tau) &= \int\int_{\Omega_{in}(\tau)} dx\, dy,\ L_{12}^{(in)}(x, y) = 1. \end{aligned}$$

The terms $A_j^{(in)}$ have to be computed, and we get:

$$\begin{aligned} A_1^{(in)} &= \int\int_{\Omega_{in}(\tau)} \frac{1}{G_2^{(in)}}\, \varphi'\left(\frac{G_1^{(in)}}{G_2^{(in)}}\right) dx\, dy = \varphi'\big(\sigma_{in}^2\big) \\ A_2^{(in)} &= \int\int_{\Omega_{in}(\tau)} \frac{-G_1^{(in)}}{\big(G_2^{(in)}\big)^2}\, \varphi'\left(\frac{G_1^{(in)}}{G_2^{(in)}}\right) dx\, dy \\ &= -\sigma_{in}^2 \varphi'\big(\sigma_{in}^2\big) \end{aligned}$$

The terms $B_{ji}^{(in)}$ also have to be computed, and we get:

$$\begin{aligned} B_{11}^{(in)} &= \int\int_{\Omega_{in}(\tau)} \frac{\partial H_1^{(in)}}{\partial K_{11}^{(in)}}\big(x, y, K_{11}^{(in)}, K_{12}^{(in)}\big)\, dx\, dy \\ &= -2\frac{1}{|\Omega_{in}|} \int\int_{\Omega_{in}(\tau)} (I(x, y) - \mu_{in}(\tau))\, dx\, dy = 0 \\ B_{12}^{(in)} &= \int\int_{\Omega_{in}(\tau)} \frac{\partial H_1^{(in)}}{\partial K_{12}^{(in)}}\big(x, y, K_{11}^{(in)}, K_{12}^{(in)}\big)\, dx\, dy \\ &= 2\frac{\mu_{in}(\tau)}{|\Omega_{in}|} \int\int_{\Omega_{in}(\tau)} (I(x, y) - \mu_{in}(\tau))\, dx\, dy = 0 \end{aligned}$$

We can then directly compute the velocity vector of the active contour from (14) and we find:

$$\begin{aligned} \frac{\partial \Gamma(\tau)}{\partial \tau} = \big[&k^{(in)} - k^{(out)} + k^{(b)} \cdot \kappa - \nabla k^{(b)} \cdot \boldsymbol{N} \\ &+ \varphi'\big(\sigma_{in}^2\big)\big((I - \mu_{in})^2 - \sigma_{in}^2\big)\big] \boldsymbol{N} \end{aligned} \qquad (15)$$

In (15), we can remark the presence of the additional term $\varphi'(\sigma_{in}^2)((I - \mu_{in})^2 - \sigma_{in}^2)\, \boldsymbol{N}$. In this term, the local intensity $I(x, y)$ appears whereas it does not appear in the descriptor itself.

3.5.2. Descriptors Depending on the Mean. We choose the following set of descriptors:

$$\begin{cases} k^{(out)} \text{ does not depend on } \tau \\ k^{(in)} = \varphi(I - \mu_{in}(\tau)) \end{cases}$$

where $\varphi(r)$ is a positive function of class C^1 ($\mathbb{R}$).

As previously, the velocity vector is computed by replacing the terms of (13) with their expressions. The descriptor $k^{(in)}$ is expressed by:

$$k^{(in)}(x, y, \tau) = g^{(in)}\big(x, y, G_1^{(in)}(\tau), G_2^{(in)}(\tau)\big) = \varphi\left(I - \frac{G_1^{(in)}(\tau)}{G_2^{(in)}(\tau)}\right)$$

where:

$$G_1^{(in)}(\tau) = \int\int_{\Omega_{in}(\tau)} H_1^{(in)}\, dx\, dy,\ H_1^{(in)} = I(x, y),$$
$$G_2^{(in)}(\tau) = \int\int_{\Omega_{in}(\tau)} H_2^{(in)}\, dx\, dy,\ H_2^{(in)} = 1,$$

In this case, the functions $H_j^{(in)}$, $j = 1, 2$ do not depend on τ and so $l_1 = l_2 = 0$ and $K_{ji}^{(in)} = 0\ \forall j\ \forall i$. The terms $A_j^{(in)}$ are then computed, and we obtain:

$$A_1^{(in)} = \int\int_{\Omega_{in}(\tau)} \frac{-1}{G_2^{(in)}}\, \varphi'\left(I - \frac{G_1^{(in)}}{G_2^{(in)}}\right) dx\, dy = \frac{-1}{|\Omega_{in}|} \int\int_{\Omega_{in}(\tau)} \varphi'(I - \mu_{in})\, dx\, dy$$
$$A_2^{(in)} = \int\int_{\Omega_{in}(\tau)} \frac{G_1^{(in)}}{\big(G_2^{(in)}\big)^2}\, \varphi'\left(I - \frac{G_1^{(in)}}{G_2^{(in)}}\right) dx\, dy = \frac{\mu_{in}}{|\Omega_{in}|} \int\int_{\Omega_{in}(\tau)} \varphi'(I - \mu_{in})\, dx\, dy$$

We can then compute directly the velocity vector of the active contour from (14) and we find:

$$\frac{\partial \Gamma(\tau)}{\partial \tau} = \left[k^{(in)} - k^{(out)} + k^{(b)} \cdot \kappa - \nabla k^{(b)} \cdot \boldsymbol{N} - \frac{(I - \mu_{in})}{|\Omega_{in}|} \int\int_{\Omega_{in}(\tau)} \varphi'(I - \mu_{in})\right] \boldsymbol{N} \tag{16}$$

Remark 1. In the particular case of $\varphi(r) = r^2$, we have $\varphi'(r) = 2r$ and therefore, the additional terms, coming from the variation of the descriptors with τ, are equal to zero as previously published by Chan and Vese (2001) and Debreuve et al. (2001).

Remark 2. However, in the general case, this additional term is not zero. For example, if $\varphi(r) = \sqrt{\varepsilon + r^2}$, with ε a positive constant, we have:

$$F = \left[k^{(in)} - k^{(out)} + k^{(b)} \cdot \kappa - \nabla k^{(b)} \cdot \boldsymbol{N} - \frac{(I - \mu_{in})}{|\Omega_{in}|} \int\int_{\Omega_{in}(\tau)} \frac{(I - \mu_{in})}{\sqrt{\varepsilon + (I - \mu_{in})^2}}\right] \tag{17}$$

Remark 3. The method has been recently successfully applied to image and segmentation using more sophisticated histogram descriptor (Aubert et al., to appear).

3.6. *Implementation Using the Level Set Method*

For numerical implementation, we can model the active contour with an explicit parameterization (Lagrangian formulation) or an implicit one (Eulerian formulation). See Sethian (1990), Osher and Sethian (1988), and Caselles et al. (1993) for more details and Delingette and Montagnat (2001) for an interesting comparison between the two methods. Another interesting review on the different methods of active contour is proposed in Montagnat et al. (2001).

The main advantages of level set methods are the accuracy and the automatic handling of topological changes while the main drawback is computational cost. However specific methods such as multiresolution, narrow band, fast marching (Sethian, 1996), additive operator splitting (Weickert et al., 1998; Goldenberg et al., 2001), have been proposed in order to speed up the level set algorithm.

In this paper we report a level set method approach, but a parametric implementation such as Precioso and Barlaud (2001) is also possible according on application requirements.

The key idea of the level set method is to introduce an auxiliary function $U(x, y, \tau)$ such that $\Gamma(\tau)$ is the zero level set of U. The function U is often chosen to be the signed distance function of $\Gamma(\tau)$, and then:

$$\Gamma(\tau) = \{(x, y)/U(x, y, \tau) = 0\}$$

This Eulerian formulation presents several advantages (Sethian, 1996). Firstly, the curve U may break or merge as the function U evolves, and topological changes are thus easily handled. Secondly, the evolving function $U(x, y, \tau)$ always remains a function allowing efficient numerical schemes. Thirdly, the geometric properties of the curve, like the curvature κ and the normal vector field $\boldsymbol{N}$, can be estimated directly from the level set function:

$$\kappa = div\left(\frac{\nabla U}{|\nabla U|}\right) \quad \text{and} \quad \boldsymbol{N} = \frac{\nabla U}{|\nabla U|}$$

The evolution equation then becomes:

$$\frac{\partial U(\tau)}{\partial \tau} = F|\nabla U| \tag{18}$$

The velocity function F is computed only on the curve $\Gamma(\tau)$ but we can extend its expression to the whole image domain Ω. To implement the level set method, solutions must be found to circumvent problems coming from the fact that the signed distance function U is not a solution of the PDE (18), see Gomes and Faugeras (2000) for details. In our work, the function U is reinitialized so that it remains a distance function, see Aubert and Kornprobst (2001) and Debreuve (2000) for details on the reinitialization equation.

In order to improve numerical efficiency, we compute the equation on a narrowband enclosing the level 0 of the level set function. We also use multiresolution techniques by making the active contour evolve first on a low resolution image. The final contour obtained for this reduced image is then used as an initial curve for the real size image.

4. Relation Between the Entropy and the Matrix Covariance Determinant

We can make the assumption that the entropy is an homogeneity descriptor since it describes the complexity of a region. For Gaussian distributions, the entropy is related to the determinant of the covariance matrix. So if we assume that each region is modelled by a Gaussian distribution, we may use the determinant of the covariance matrix as an homogeneity descriptor. In this section, we first recall the relation between entropy and covariance matrix determinant.

The entropy of a random vector $\mathbf{X} = (X^1, X^2, X^3, \ldots, X^n)$ of probability distribution f_X is defined as:

$$S(\mathbf{X}) = -\int f_{\mathbf{x}}(\mathbf{x}) \ \ln \ f_{\mathbf{x}}(\mathbf{x}) \, d\mathbf{x}$$

In the case of a multidimensional Gaussian distribution, of dimension n, of mean μ and covariance matrix Σ, we have:

$$f_{\mathbf{x}}(\mathbf{x}) = \frac{1}{(2\pi)^{n/2}(\det(\Sigma))^{1/2}} \times \exp\left[-\frac{1}{2}(\mathbf{x}-\mu)^T \Sigma^{-1}(\mathbf{x}-\mu)\right],$$

and we can prove that the entropy S depends on the determinant of the covariance matrix with the following equation (the proof can be found in Gray and Davidson (2000)):

$$S = \frac{1}{2}\ln[(2\pi e)^n \det(\Sigma)] \tag{19}$$

The intensity for color images is represented by a function $\mathbf{I} : \Omega \subset \mathbb{R}^2 \to \mathbb{R}^3$ where $\mathbf{I} = [I^1, I^2, I^3]^T$. As far as the segmentation of homogeneous color regions is concerned, we may assume that each color region R_k is modelled by a Gaussian distribution of mean $\mu_{\mathbf{k}} = [\mu_k^1, \mu_k^2, \mu_k^3]^T$ and covariance matrix Σ_k. The probability density function is given by the following expression:

$$p(\mathbf{I}(\mathbf{x}) \in R_k/(\mu_{\mathbf{k}}, \Sigma_k)) = \frac{1}{(2\pi)^{3/2}(\det(\Sigma_k))^{1/2}} \times \exp\left[-\frac{1}{2}(\mathbf{I}-\mu_{\mathbf{k}})^T \Sigma_k^{-1}(\mathbf{I}-\mu_{\mathbf{k}})\right]$$

We thus deduce for the entropy S_{R_k} of the region R_k:

$$S_{R_k} = \frac{1}{2}\ln[(2\pi e)^3 \det(\Sigma_k)] \tag{20}$$

So, minimizing the determinant of the covariance matrix means that we want to decrease the complexity of a region (Gray et al., 2001; Pateux, 2000). In the following, we choose this quantity as a powerful descriptor for the segmentation of homogeneous regions. Let us first study the variance as a descriptor for the segmentation of homogeneous regions in greyscale images, in order to point out the importance of the additional terms computed in Section 3.5.

5. Segmentation of Homogeneous Regions Based on a Competition Between the Variances for Greyscale Images

In this section, we propose some region-dependent descriptors to segment homogeneous regions on greyscale images. These descriptors are based on the minimization of the variances of the two considered regions. In the second part, the importance of the additional terms, coming from the variation of the descriptors with the evolving regions, is highlighted.

5.1. Descriptor Based on the Variance for Greyscale Images

The intensity for greyscale images is represented by a function $\boldsymbol{I} : \Omega \subset \mathbb{R}^2 \to \mathbb{R}$. We propose to minimize the variances of the two considered homogeneous regions in order to segment them. The following descriptors are suggested:

$$\begin{cases} k^{(out)} = \varphi\left(\sigma_{out}^2\right) \\ k^{(in)} = \varphi\left(\sigma_{in}^2\right) \\ k^{(b)} = \lambda \end{cases}$$

where $\varphi(r)$ is a positive function of class $C^1(\mathbb{R})$ and λ a positive constant.

The computation of the velocity vector is deduced from the computation of the derivative of the criterion J developed in Section 3.5.1, which leads to the following evolution equation:

$$\frac{\partial \Gamma(\tau)}{\partial \tau} = \left[\varphi\left(\sigma_{in}^2\right) - \varphi\left(\sigma_{out}^2\right) + \lambda\kappa + \varphi'\left(\sigma_{in}^2\right)\left((I - \mu_{in})^2 - \sigma_{in}^2\right) - \varphi'\left(\sigma_{out}^2\right)\left((I - \mu_{out})^2 - \sigma_{out}^2\right)\right]\boldsymbol{N} \tag{21}$$

The single parameter we need to adjust is the smoothing parameter λ. In fact, the flow $[\lambda\kappa]$ has the properties of smoothing because it moves the curve in the direction of a minimal length (Siddiqi et al., 1996).

5.2. Experimental Results

We make the active contour evolve on a synthetic image composed by an homogeneous square of intensity 100 on a background of intensity 160. A Gaussian noise of variance 20 is added to this synthetic image. For the experiments, we take $\varphi(r) = \log(1 + r)$ which gives $\varphi'(r) = 1/(1 + r)$ and we choose $\lambda = 10$.

5.2.1. Importance of the Additional Region Based Terms. In order to evaluate the importance of the additional terms for the segmentation, we make the active contour evolve through the PDE (21), including the additional terms and we also make it evolve with the following approximate evolution equation that does not include the additional terms:

$$\frac{\partial \Gamma(\tau)}{\partial \tau} = \left[\varphi\left(\sigma_{in}^2\right) - \varphi\left(\sigma_{out}^2\right) + \lambda\kappa\right]\boldsymbol{N} \tag{22}$$

The evolution of the active contour driven by (21) is given in Fig. 3 while the one obtained using (22) is given in Fig. 4. We can remark that when the PDE includes the additional terms, the square is well segmented (Fig. 3(c)), whereas when the PDE does not include these additional terms we obtain a circle instead of the expected square (Fig. 4(c)). These results can be better understood while analyzing the velocity vectors of each evolution equation. We compare the two evolutions of the velocity vectors using PDE (21) during the propagation of the curve. The evolution of the amplitude is given in Fig. 3(d–f), while the amplitude using PDE (22) is given in Fig. 4(d–f). We can observe that the velocity using PDE (22) is a constant where obviously the image features do not appear. On the contrary the image features well appear in the velocity using PDE (21) and so the square can be well segmented.

5.2.2. Estimation of the Variances and the Means. The variances and the means of each region evolve during the segmentation process. At convergence, these parameters are estimated for each region. Indeed, we jointly perform segmentation and estimation. The evolution of the means of each region in the course of the iterations is given Fig. 5. At the end of the process, we obtain $\mu_{in} = 160$ and $\mu_{out} = 100$ and so these parameters are correctly estimated. The evolution of the variances during the process are given Fig. 6. Both variances evolve towards the value 20, which is correct since a Gaussian noise of variance 20 has been added to the synthetic image.

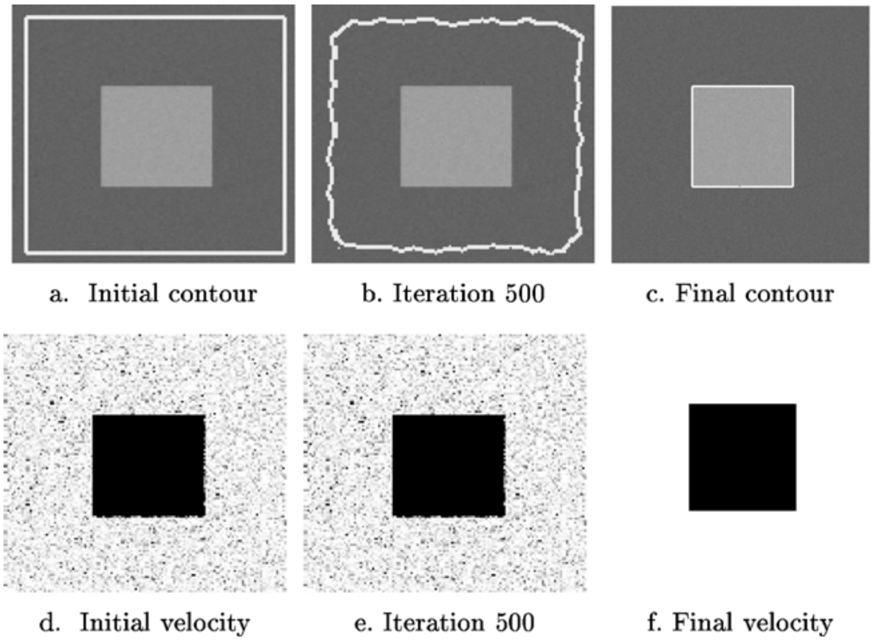

Figure 3. Figures (a)–(c): Evolution of the active contour managed by the PDE including the additional terms. Figures (d)–(f): Visualization of the corresponding velocity function including the additional terms normalized between 0 and 255, such that the negative values are lower than 128 and the positive ones are higher than 128.

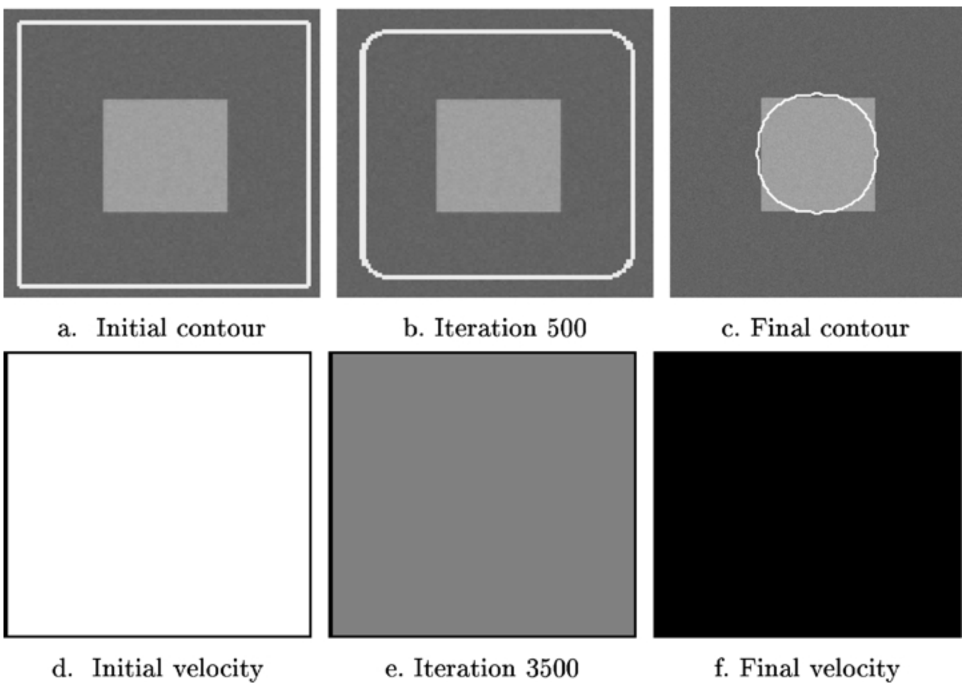

Figure 4. Figures (a)–(c): Evolution of the active contour managed by the PDE without the additional terms (Figs. (a)–(c)). Figures (d)–(f): Visualization of the corresponding velocity function, without the additional terms (normalized such that max = 255).

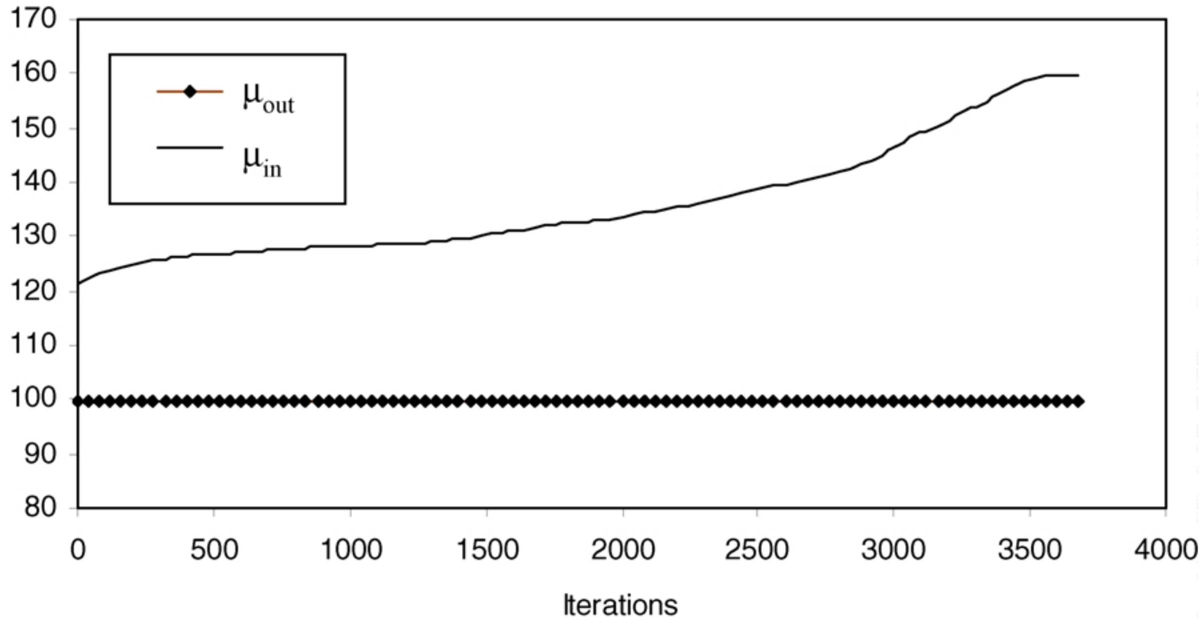

Figure 5. Evolution of the means of Ω_{in} and Ω_{out} during the segmentation process of the "square".

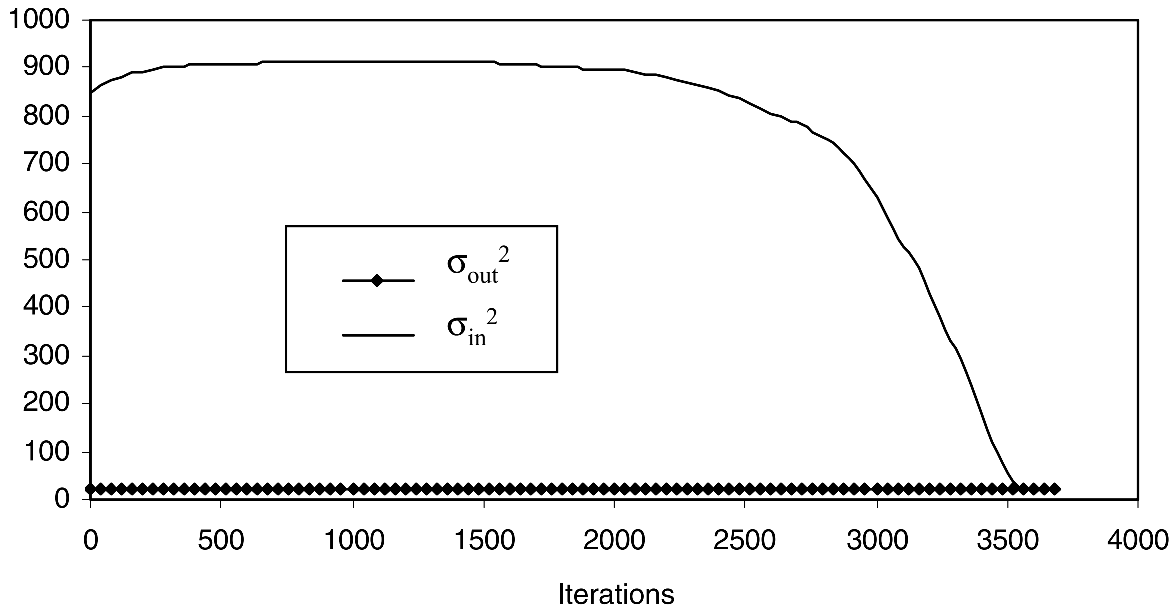

Figure 6. Evolution of the variances of Ω_{in} and Ω_{out} during the segmentation process of the "square".

6. Segmentation of Color Homogeneous Regions Based on the Covariance Matrix: Application to Face Detection in Video Sequences

This part deals with the segmentation of homogeneous regions in multispectral images. We choose the determinant of the covariance matrix as a descriptor to segment homogeneous color regions in reason of its link with entropy given Section 4. This tool may practically be used for face segmentation in image sequences.

6.1. Descriptors Based on the Covariance Matrix for Color Images

Let us denote by Σ_{in} and Σ_{out} the covariance matrix of respectively $\Omega_{in}(\tau)$ and $\Omega_{out}(\tau)$:

$$\Sigma_{.} = \begin{pmatrix} \sigma_{.}^{11} & \sigma_{.}^{12} & \sigma_{.}^{13} \\ \sigma_{.}^{21} & \sigma_{.}^{22} & \sigma_{.}^{23} \\ \sigma_{.}^{31} & \sigma_{.}^{32} & \sigma_{.}^{33} \end{pmatrix}$$

where:

$$\begin{cases} \sigma_{.}^{ij} = \dfrac{1}{|\Omega_{.}|} \displaystyle\iint_{\Omega_{.}(\tau)} (I^i - \mu_{.}^i) \\ \qquad \times (I^j - \mu_{.}^j)\, dx\, dy \qquad\qquad \text{with } \cdot = in \text{ or } out \\ \mu_{.}^i = \dfrac{1}{|\Omega_{.}|} \displaystyle\iint_{\Omega_{.}(\tau)} I^i(x, y)\, dx\, dy \end{cases}$$

We obviously have $\sigma_{.}^{ij} = \sigma_{.}^{ji}$. Let us denote by $\det(\Sigma_{.})$ the determinant of the covariance matrix which expression is the following:

$$\det(\Sigma_{.}) = \sigma_{.}^{11}\sigma_{.}^{22}\sigma_{.}^{33} + 2\sigma_{.}^{12}\sigma_{.}^{13}\sigma_{.}^{23} - \sigma_{.}^{11}\sigma_{.}^{23}\sigma_{.}^{23} - \sigma_{.}^{22}\sigma_{.}^{13}\sigma_{.}^{13} - \sigma_{.}^{33}\sigma_{.}^{12}\sigma_{.}^{12} \tag{23}$$

Functions of the covariance matrix determinants are used as region descriptors. We choose the following set of descriptors:

$$\begin{cases} k^{(out)} = \Phi(\det(\Sigma_{out})) \\ k^{(in)} = \Phi(\det(\Sigma_{in})) \\ k^{(b)} = \lambda \end{cases}$$

where $\Phi(r)$ is a positive function of class $C^1(\mathbb{R})$ and λ a positive constant. Let us now write the evolution equation of the active contour by computing the different terms of (13). Details of the computation can be found in Appendix B. The evolution equation of the active contour is the following:

$$\begin{aligned} \frac{\partial \Gamma(\tau)}{\partial \tau} = \Bigg[& \Phi(\det(\Sigma_{in})) - \Phi(\det(\Sigma_{out})) + \lambda\kappa \\ & + \Phi'(\det(\Sigma_{in})) \Bigg[\sum_{k,l=1}^{3} \big(I^k - \mu_{in}^k\big)\big(I^l - \mu_{in}^l\big) \\ & \times \det\big(M_{in}^{kl}\big)(-1)^{k+l} \Bigg] - 3\det(\Sigma_{in})\Phi'(\det(\Sigma_{in})) \\ & - \Phi'(\det(\Sigma_{out})) \Bigg[\sum_{k,l=1}^{3} \big(I^k - \mu_{out}^k\big) \\ & \times \big(I^l - \mu_{out}^l\big)\det\big(M_{out}^{kl}\big)(-1)^{k+l} \Bigg] \\ & + 3\det(\Sigma_{out})\Phi'(\det(\Sigma_{out})) \Bigg] N \end{aligned} \tag{24}$$

The matrix $M_{.}^{kl}$ is deduced from the covariance matrix $\Sigma_{.}$ by suppressing the k^{th} row and the l^{th} column. The last four lines of the equation are the additional terms coming from the variation of the descriptors with τ. As it has been previously demonstrated for greyscale images, these terms have to be considered in order to make the active contour converge towards a minimum of the criterion.

6.2. Experimental Results

For the experiments, we take $\varphi(r) = \log(1 + r)$ which gives $\varphi'(r) = 1/(1 + r)$ and $\Phi(r) = \log(1 + r^2)$ which gives $\Phi'(r) = 2r/(1 + r^2)$. We choose $\lambda = 15$. The color space selected is (Y, U, V), where $(I^1 = Y)$ represents the luminance and $(I^2 = U)$ and $(I^3 = V)$ represent the two chrominances. For the computation of the variance, only the luminance is used.

6.2.1. Segmentation of a Region. In order to segment an homogeneous region, we start with an initial curve inside the region of interest. The curve is then supposed to expand until it reaches the boundary of the concerned homogeneous region.

The algorithm based on the covariance matrix is performed on an image of the video sequence “erik” in order to detect the speaker’s face. The evolution of the curve is given in Fig. 7. The contour evolves to finally

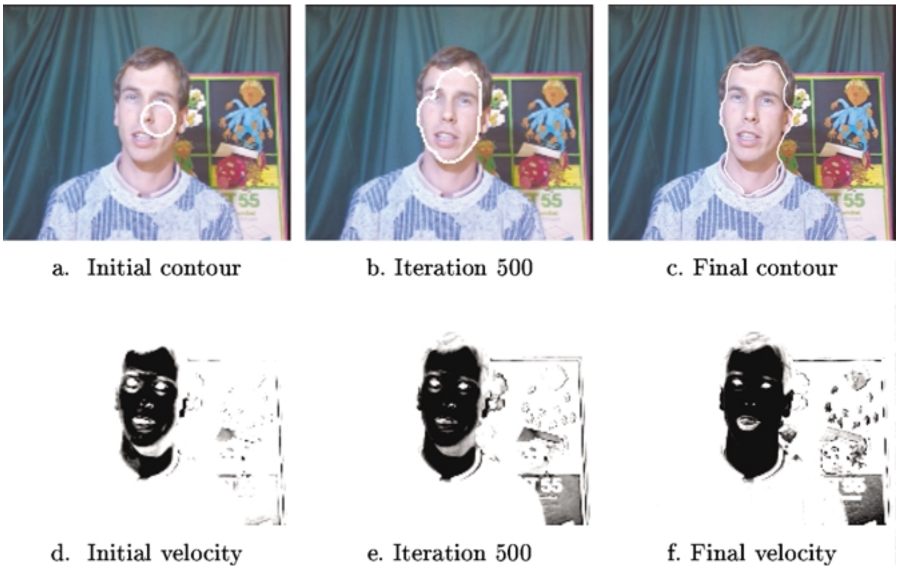

Figure 7. Visualization of the evolution of the contour and the velocity (without the boundary-based term) for the segmentation of the face using the covariance matrix.

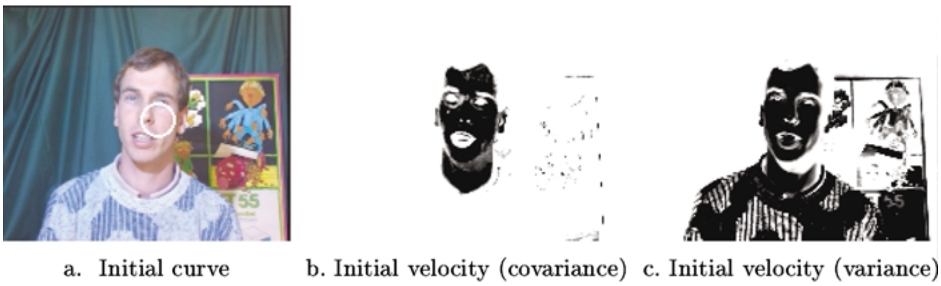

Figure 8. Comparison of the initial velocity computed using the covariance matrix (Fig. (b)) to the one computed using the variance (Fig. (c)) from the same initial curve (Fig. (a)).

Figure 9. Evolution of the curve from the initial curve (a) using the evolution Eq. (25) without the additive terms coming from the derivation of the determinant of the covariance matrix ($\lambda = 15$).

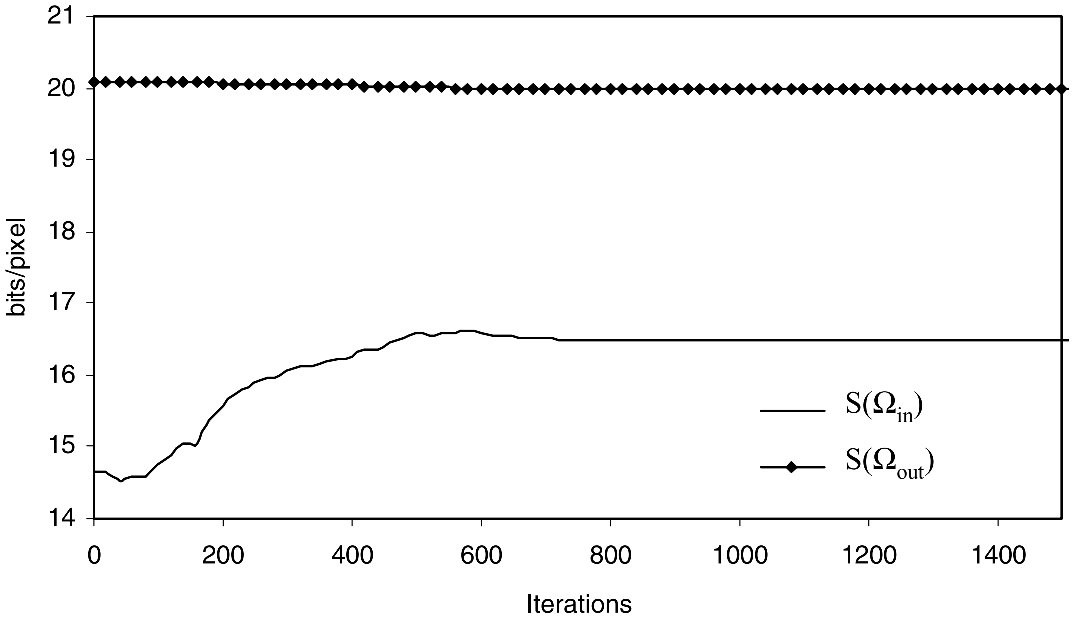

Figure 10. Evolution of the entropy during the segmentation process computed using its relation with the determinant of the covariance matrix given in Eq. (20).

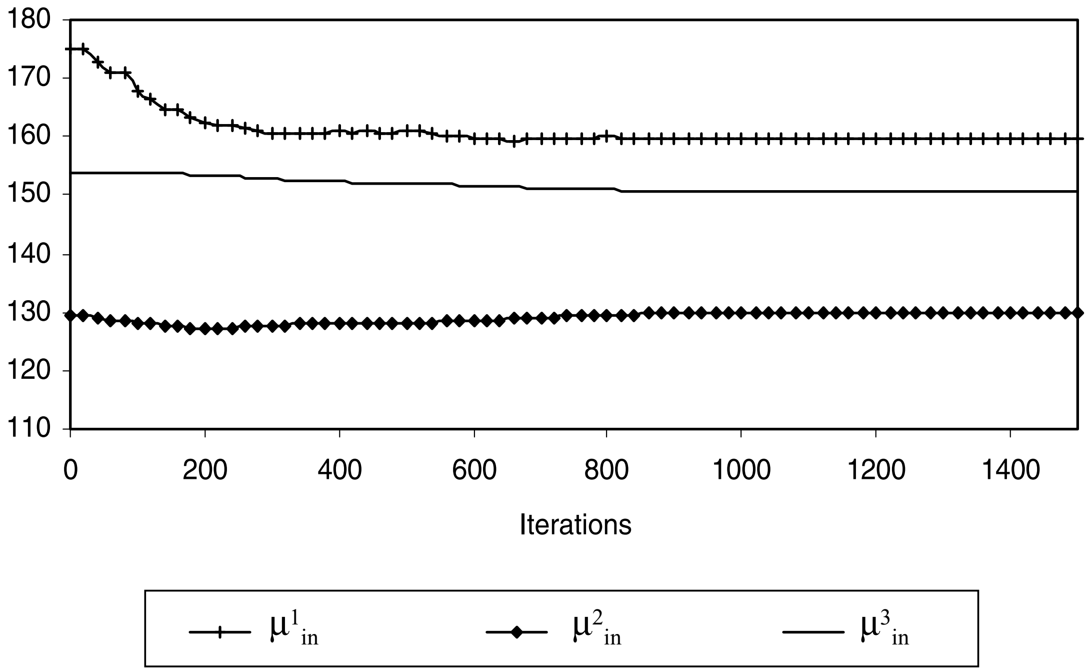

Figure 11. Evolution of the mean μ_{in} during the segmentation process for an image of the video sequence "erik".

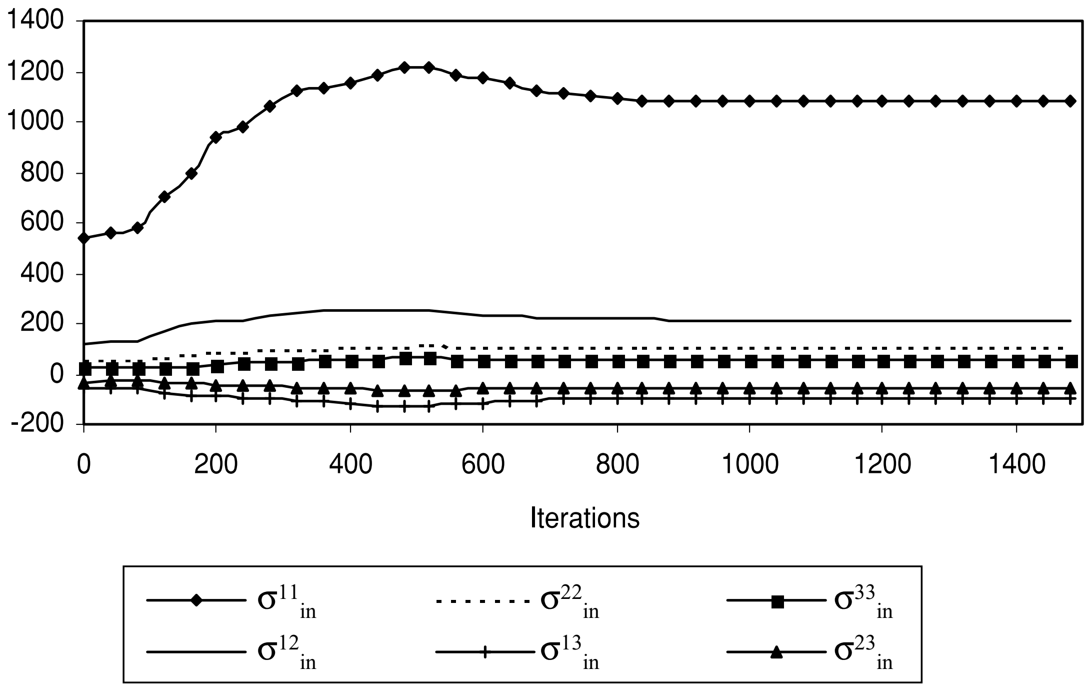

Figure 12. Evolution of the variances and the covariances of Ω_{in} during the segmentation process for an image of the video sequence "erik".

converge on the boundaries of the face (Fig. 7(c)). The face is then accurately segmented. The amplitude of the velocity is also given in Fig. 7(d–f) and we can observe that the face region is very well delimited from the other regions. The velocity given in Fig. 7(d–f) includes the additional terms coming from the variation of the descriptors with τ. Althougth we use a boundary based term in the velocity, it is not included in the velocity field given in this figure. The amplitude of the velocity is normalized between 0 and 255, such that the negative values are lower than 128 and the positive ones are higher than 128.

6.2.2. Comparison of the Velocities Obtained Using the Variance and Using the Determinant of the Covariance Matrix. We can compare the initial velocity obtained using the covariance matrix (24) with the one obtained using the variance (21). The face is not well-detected in the velocity obtained using the variance (Fig. 8(c)) whereas it is really well-detected in the initial velocity using the covariance matrix (Fig. 8(b)). The velocity obtained using the variance does not allow an efficient segmentation of the face on the contrary to the determinant of the covariance matrix which takes advantage of the color information.

6.2.3. Importance of the Additional Terms. As previously described for the descriptor based on the variance, we can make the contour evolve using the following PDE without the additional terms:

$$\frac{\partial \Gamma(\tau)}{\partial \tau} = [\Phi(\det(\Sigma_{in})) - \Phi(\det(\Sigma_{out})) + \lambda\kappa]\boldsymbol{N} \quad (25)$$

The results of the segmentation process are given Fig. 9. We can remark that the face is not correctly segmented.

6.2.4. Estimation. The determinant of the covariance matrix is a region-dependent descriptor which evolves during the propagation of the curve. At convergence, this parameter is estimated for both regions Ω_{in} and Ω_{out}. We can thus estimate the entropy of each region using the relation (20). The results are given in Fig. 10. The values are computed in *bits/pixel*. We can remark that the entropy of Ω_{out}, namely $S(\Omega_{out})$ decreases slowly while the entropy of Ω_{in}, namely $S(\Omega_{in})$ increases.

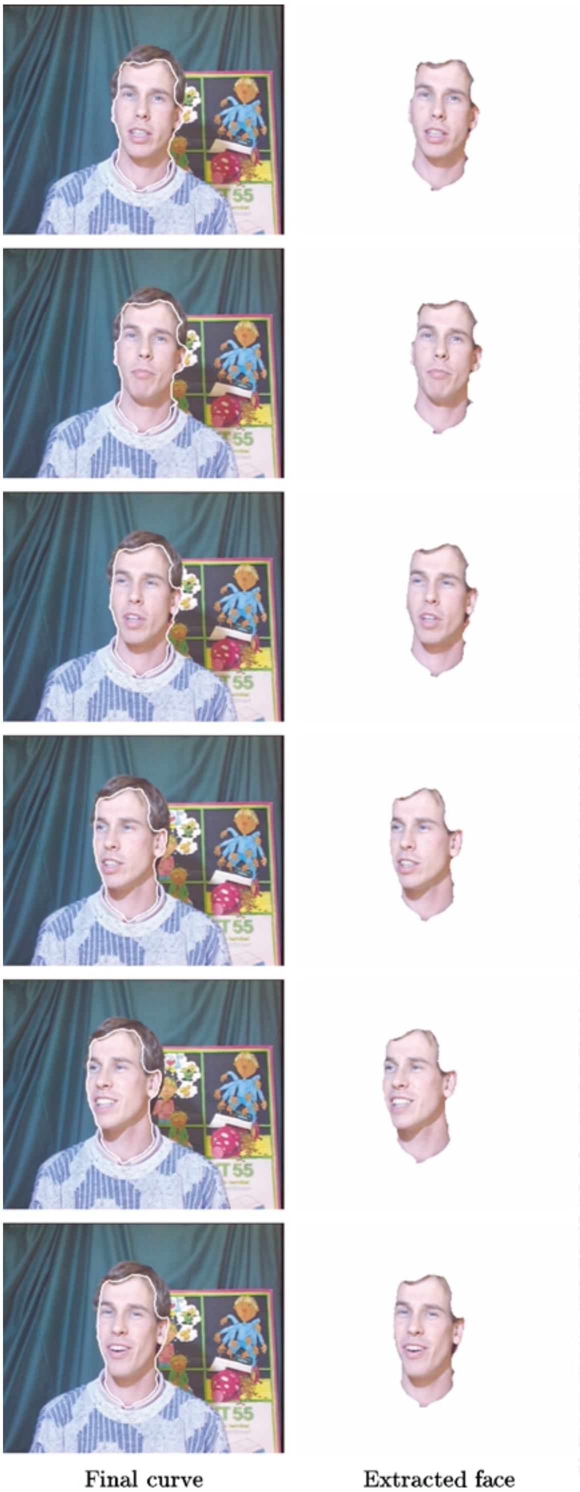

Figure 13. Detection of the face on the video sequence "erik".

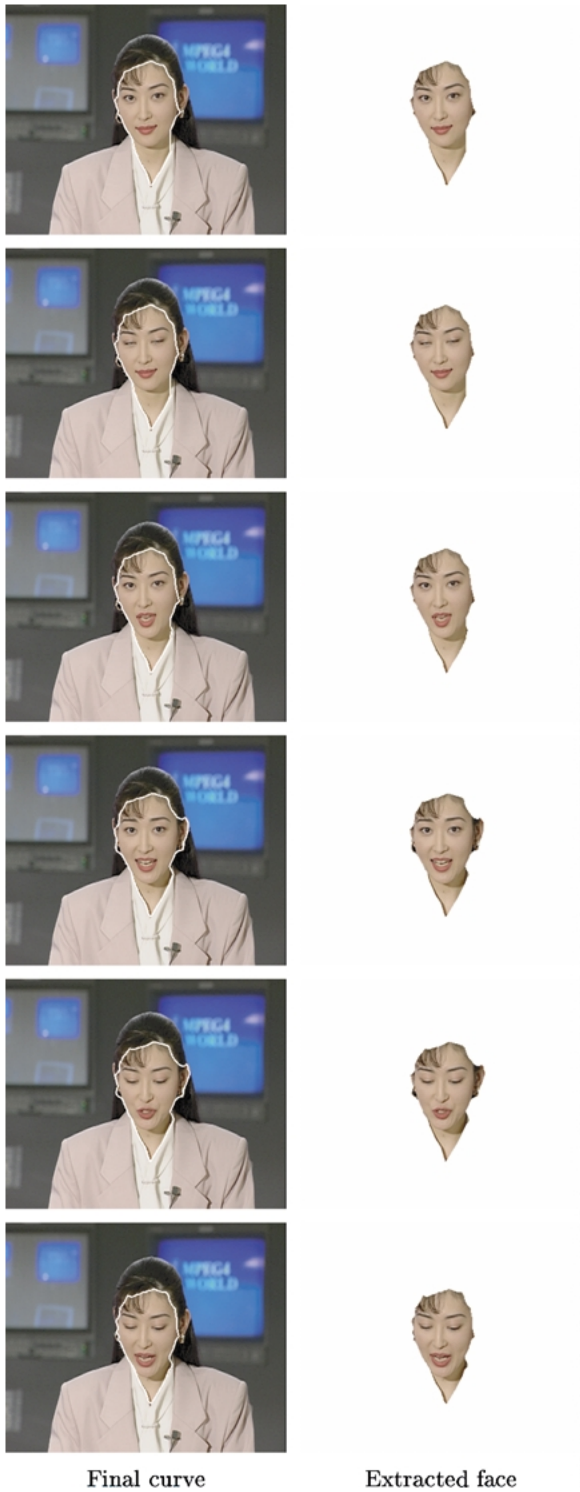

Figure 14. Detection of the face on the video sequence "akiyo".

The means, the variances and the covariances of each region are also estimated. We show the evolution of these parameters for the region Ω_{in} in Figs. 11 and 12.

6.3. Application to Face Segmentation in Video Sequences

The descriptors based on the covariance matrix are implemented to segment human faces in video sequences. This segmentation may be used for video coding to encode selectively the human face. For a given compression ratio, the face can be transmitted with a higher rate to the detriment of the background. This interesting property is valuable for videoconferences, where the most important and most variable information is located on the face, see for example Amonou and Duhamel (2000) and Salembier (1994). Face segmentation may also be used for high level applications as face and person recognition, biometry, indexing and retrieval (MPEG-7, 1998; MPEG-7, 2000).

We initialize the first frame with a circle inside the face to track. Then, we make the active contour evolve using (24), with $\Phi(r) = \log(1 + r^2)$. The final contour of the current image is then chosen as an initial curve for the next image. The algorithm has been performed on several sequences. The results for the sequence "erik" are given in Fig. 13. The parameter λ has been set to 15. The face is well detected and tracked on the whole sequence. The results for the sequence "akiyo" are given in Fig. 14. We choose $\lambda = 20$. We can see that the face is well detected even if the color of her shirt is close to the face color.

7. Conclusion

In this paper, we propose a new Eulerian minimization method to compute the velocity vector of an active contour that ensures its evolution towards a minimum of a criterion including both region-based and boundary-based terms. Our approach is based on shape optimization methods and is performed in three main steps:

1. Introduction of a dynamical scheme in the criterion,
2. Computation of the Eulerian derivative of the criterion using shape optimization tools,
3. Computation of the evolution equation of the active contour from the derivative.

DREAM^{2}S allows to readily take into account the case of region-dependent descriptors that are globally attached to the evolving regions. We show that the variation of these descriptors induces additional terms in the velocity equation of the active contour. Some examples are taken showing that these additional terms induce local terms in the evolution equation. Besides, region-dependent descriptors evolve during the propagation of the curve to finally converge, allowing to jointly perform segmentation and estimation.

For color regions segmentation, we propose to minimize the entropy through the covariance matrix determinant. The covariance matrix determinant is then chosen as a statistical region-dependent descriptor. It appears to be a very powerful tool for homogeneous regions segmentation and it has been successfully applied to face segmentation in video sequences.

The method has been recently successfully applied to histogram descriptors that fit exactly to the data (Aubert et al., to appear).

Appendix A

The issue is to differentiate the following domain functional:

$$J(\Omega_i) = \int\int_{\Omega_i} k_i(x, y, \Omega_i)\, dx\, dy$$

Since the set of all domains has not a structure of vectorial space, let us make the regions evolve through a family of transformations $(T(\tau, \cdot))_{\tau\geq 0}$ smooth and bijective. For a point $p = [x, y]^T$, we note:

$$p(\tau) = T(\tau, p) \quad \text{with} \quad T(0, p) = p$$
$$\Omega_i(\tau) = T(\tau, \Omega_i) \quad \text{with} \quad T(0, \Omega_i) = \Omega_i$$

Let us then define the velocity vectors field $\boldsymbol{V}$ such that:

$$\boldsymbol{V}(\tau, p(\tau)) = \frac{\partial T}{\partial \tau}(\tau, p)$$

As far as the computation of the derivative is concerned, we are interested in small deformations. We thus expand the transformation according to first order Taylor formula:

$$T(\tau, p) = T(0, p) + \tau \frac{\partial T}{\partial \tau}(0, p) = p + \tau \boldsymbol{V}(p)$$

where $\boldsymbol{V}(p) = \frac{\partial T}{\partial \tau}(0, p)$.

We then introduce three main definitions (Sokolowski and Zolésio, 1992; Delfour and Zolésio, 2001):

1. The Eulerian derivative of $J(\Omega_i)$ (in the direction of $\boldsymbol{V}$):

$$dJ(\Omega_i, \boldsymbol{V}) = \lim_{\tau \to 0} \frac{J(\Omega_i(\tau)) - J(\Omega_i)}{\tau} \tag{26}$$

2. The material derivative of $k_i(p, \Omega_i)$:

$$\dot{k}_i(p, \Omega_i, \boldsymbol{V}) = \lim_{\tau \to 0} \frac{k_i(p + \tau \boldsymbol{V}(p), \Omega_i + \tau \boldsymbol{V}(p)) - k_i(p, \Omega_i)}{\tau} \tag{27}$$

3. The shape derivative of $k_i(p, \Omega_i)$:

$$k_i'(p, \Omega_i, \boldsymbol{V}) = \lim_{\tau \to 0} \frac{k_i(p, \Omega_i + \tau \boldsymbol{V}(p)) - k_i(p, \Omega_i)}{\tau} \tag{28}$$

Obviously, by expanding (27) according to first order Taylor formula, we have:

$$\dot{k}_i(p, \Omega_i, \boldsymbol{V}) = k_i'(p, \Omega_i, \boldsymbol{V}) + \nabla k_i(p, \Omega_i) \cdot \boldsymbol{V}(p) \tag{29}$$

We then compute more precisely the Eulerian derivative of $J(\Omega_i)$. We have:

$$\frac{J(\Omega_i(\tau)) - J(\Omega_i)}{\tau} = \frac{1}{\tau}\left[\int\int_{\Omega_i(\tau)} k_i(p(\tau), \Omega_i(\tau))\, dp - \int\int_{\Omega_i} k_i(p, \Omega_i)\, dp\right] \tag{30}$$

In the first integral, we make the variable change $p(\tau) = p + \tau \boldsymbol{V}(p)$ where $\boldsymbol{V}(p) = [V_1(x, y), V_2(x, y)]^T$, which gives:

$$\int\int_{\Omega_i(\tau)} k_i(p(\tau), \Omega_i(\tau))\, dp = \int\int_{\Omega_i} k_i(p + \tau \boldsymbol{V}(p), \Omega_i + \tau \boldsymbol{V}(p)) |\det J_\tau(p)|\, dp \tag{31}$$

where $J_\tau(p)$ is the following Jacobian matrix:

$$J_\tau(p) = \begin{pmatrix} 1 + \tau \frac{\partial V_1}{\partial x} & \tau \frac{\partial V_1}{\partial y} \\ \tau \frac{\partial V_2}{\partial x} & 1 + \tau \frac{\partial V_2}{\partial y} \end{pmatrix}$$

and so, we have:

$$\det J_\tau(p) = 1 + \tau \operatorname{div}(\boldsymbol{V}(p)) + \tau^2 \det(\nabla \boldsymbol{V}(p))$$

Then we obtain:

$$\lim_{\tau \to 0} \frac{\det J_\tau(p) - 1}{\tau} = \operatorname{div}(\boldsymbol{V}(p)) \tag{32}$$

The Eq. (30) then becomes:

$$\frac{J(\Omega_i(\tau)) - J(\Omega_i)}{\tau} = \frac{1}{\tau}\left[\int\int_{\Omega_i} k_i(p + \tau \boldsymbol{V}(p), \Omega_i + \tau \boldsymbol{V}(p)) |\det J_\tau(p)|\, dp - \int\int_{\Omega_i} k_i(p, \Omega_i)\, dp\right] \tag{33}$$

We can suppose that $\det(J_\tau(p)) \neq 0\ \forall \tau\ \forall p$. We may then take $\det(J_\tau(p)) > 0$, and we develop the expression (33) as following by adding a term in the second integral while suppressing the same term in the first integral:

$$\frac{J(\Omega_i(\tau)) - J(\Omega_i)}{\tau} = I_1 + I_2 \tag{34}$$

where:

$$I_1 = \int\int_{\Omega_i} \frac{k_i(p + \tau \boldsymbol{V}(p), \Omega_i + \tau \boldsymbol{V}(p)) - k_i(p, \Omega_i)}{\tau} \times \det(J_\tau(p))\, dp \tag{35}$$

$$I_2 = \int\int_{\Omega_i} k_i(p, \Omega_i) \frac{\det(J_\tau(p)) - 1}{\tau}\, dp \tag{36}$$

Let us make τ tend towards 0. Using (29) and Definitions (27, 28), we get:

$$\begin{aligned}
\lim_{\tau\to 0} I_1 &= \int\int_{\Omega_i} \dot{k}_i(p, \Omega_i, \boldsymbol{V})\, dp \\
&= \int\int_{\Omega_i} k_i'(p, \Omega_i, \boldsymbol{V})\, dp \\
&\quad + \int\int_{\Omega_i} \nabla k_i(p, \Omega_i) \cdot \boldsymbol{V}(p)\, dp \\
\lim_{\tau\to 0} I_2 &= \int\int_{\Omega_i} k_i(p, \Omega_i) \mathrm{div}(\boldsymbol{V})\, dp
\end{aligned}$$

And so for the Eulerian derivative, we find:

$$\begin{aligned}
dJ(\Omega_i, \boldsymbol{V}) &= \int\int_{\Omega_i} k_i'(p, \Omega_i, \boldsymbol{V})\, dp \\
&+ \int\int_{\Omega_i} (\nabla k_i(p, \Omega_i) \cdot \boldsymbol{V}(p) + k_i(p, \Omega_i)\mathrm{div}(\boldsymbol{V}(p)))\, dp \\
&= \int\int_{\Omega_i} k_i'(p, \Omega_i, \boldsymbol{V})\, dp \\
&+ \int\int_{\Omega_i} \mathrm{div}(k_i\, \boldsymbol{V})\, dp
\end{aligned} \tag{37}$$

When applying the Green-Riemann theorem in (37), we finally obtain:

$$\begin{aligned}
dJ(\Omega_i, \boldsymbol{V}) &= \int\int_{\Omega_i} k_i'(p, \Omega_i, \boldsymbol{V})\, dp \\
&\quad - \int_{\partial\Omega_i} k_i\big(\boldsymbol{V} \cdot \boldsymbol{N}_{\partial\Omega_i}\big)\, ds
\end{aligned} \tag{38}$$

where $\boldsymbol{N}_{\partial\Omega_i}$ is the unit inward normal to $\partial\Omega_i$. The Eulerian derivative is noted $J'(\tau)$ in the paper and the shape derivative k_i' is noted $\frac{\partial k_i}{\partial\tau}$.

Remark. For simplicity, we choose the following variation in the proof: $p(\tau) = p + \tau\boldsymbol{V}(p)$. The proof may also be developed with more general variations such as: $p(\tau) = f(p, \tau)$ with f a smooth function and $f(\cdot, \tau)$ bijective.

Appendix B

We have to compute the different terms of (14) in order to obtain the evolution equation of the active contour for the descriptors based on the determinant of the covariance matrix. The computation is performed for the descriptor $k^{(in)}$. Obviously, a similar computation can be done for $k^{(out)}$. We can express $k^{(in)}$ as a combination of functions depending on the region Ω_{in}:

$$k^{(in)}(x, y, \tau) = g\left(\frac{Z^{(in)}}{\big(G_7^{(in)}\big)^2}\right)$$

where $g = \Phi$, with Φ the function defined previously, and:

$$\begin{aligned}
Z^{(in)} &= G_1^{(in)} G_2^{(in)} G_3^{(in)} + 2G_4^{(in)} G_5^{(in)} G_6^{(in)} \\
&\quad - G_1^{(in)}\big(G_6^{(in)}\big)^2 - G_2^{(in)}\big(G_5^{(in)}\big)^2 - G_3^{(in)}\big(G_4^{(in)}\big)^2
\end{aligned}$$

with:

$$\begin{cases}
G_1^{(in)} = \int\int_{\Omega_{in}(\tau)} \big(I^1 - \mu_{in}^1\big)^2\, dx\, dy \\
G_2^{(in)} = \int\int_{\Omega_{in}(\tau)} \big(I^2 - \mu_{in}^2\big)^2\, dx\, dy \\
G_3^{(in)} = \int\int_{\Omega_{in}(\tau)} \big(I^3 - \mu_{in}^3\big)^2\, dx\, dy \\
G_4^{(in)} = \int\int_{\Omega_{in}(\tau)} \big(I^1 - \mu_{in}^1\big)\big(I^2 - \mu_{in}^2\big)\, dx\, dy \\
G_5^{(in)} = \int\int_{\Omega_{in}(\tau)} \big(I^1 - \mu_{in}^1\big)\big(I^3 - \mu_{in}^3\big)\, dx\, dy \\
G_6^{(in)} = \int\int_{\Omega_{in}(\tau)} \big(I^2 - \mu_{in}^2\big)\big(I^3 - \mu_{in}^3\big)\, dx\, dy \\
G_7^{(in)} = \int\int_{\Omega_{in}(\tau)} dxdy
\end{cases}$$

And so the functions $H_j^{(in)}$ have the following expressions:

$$\begin{cases}
H_1^{(in)} = \big(I^1 - \mu_{in}^1\big)^2 \\
H_2^{(in)} = \big(I^2 - \mu_{in}^2\big)^2 \\
H_3^{(in)} = \big(I^3 - \mu_{in}^3\big)^2 \\
H_4^{(in)} = \big(I^1 - \mu_{in}^1\big)\big(I^2 - \mu_{in}^2\big) \\
H_5^{(in)} = \big(I^1 - \mu_{in}^1\big)\big(I^3 - \mu_{in}^3\big) \\
H_6^{(in)} = \big(I^2 - \mu_{in}^2\big)\big(I^3 - \mu_{in}^3\big) \\
H_7^{(in)} = 1
\end{cases}$$

From these expressions, as it has been performed for the variance in Section 3.5.1, we easily deduce that:

$$B_{ji}^{(in)} = 0 \quad \forall j\ \forall i$$

We then have to compute the terms $A_j^{(in)}$ from the expressions of $G_j^{(in)}$, which leads to:

$$\begin{cases} A_1^{(in)} = \displaystyle\int\int_{\Omega_{in}(\tau)} \frac{\partial g}{\partial G_1^{(in)}} = \int\int_{\Omega_{in}(\tau)} \frac{G_2^{(in)}G_3^{(in)} - \left(G_6^{(in)}\right)^2}{\left(G_7^{(in)}\right)^3}\Phi'(\det(\Sigma_{in})) \\ A_2^{(in)} = \displaystyle\int\int_{\Omega_{in}(\tau)} \frac{\partial g}{\partial G_2^{(in)}} = \int\int_{\Omega_{in}(\tau)} \frac{G_1^{(in)}G_3^{(in)} - \left(G_5^{(in)}\right)^2}{\left(G_7^{(in)}\right)^3}\Phi'(\det(\Sigma_{in})) \\ A_3^{(in)} = \displaystyle\int\int_{\Omega_{in}(\tau)} \frac{\partial g}{\partial G_3^{(in)}} = \int\int_{\Omega_{in}(\tau)} \frac{G_1^{(in)}G_2^{(in)} - \left(G_4^{(in)}\right)^2}{\left(G_7^{(in)}\right)^3}\Phi'(\det(\Sigma_{in})) \\ A_4^{(in)} = \displaystyle\int\int_{\Omega_{in}(\tau)} \frac{\partial g}{\partial G_4^{(in)}} = \int\int_{\Omega_{in}(\tau)} \frac{-2\left(G_3^{(in)}G_4^{(in)} - G_5^{(in)}G_6^{(in)}\right)}{\left(G_7^{(in)}\right)^3}\Phi'(\det(\Sigma_{in})) \\ A_5^{(in)} = \displaystyle\int\int_{\Omega_{in}(\tau)} \frac{\partial g}{\partial G_5^{(in)}} = \int\int_{\Omega_{in}(\tau)} \frac{2\left(G_4^{(in)}G_6^{(in)} - G_2^{(in)}G_5^{(in)}\right)}{\left(G_7^{(in)}\right)^3}\Phi'(\det(\Sigma_{in})) \\ A_6^{(in)} = \displaystyle\int\int_{\Omega_{in}(\tau)} \frac{\partial g}{\partial G_6^{(in)}} = \int\int_{\Omega_{in}(\tau)} \frac{-2\left(G_1^{(in)}G_6^{(in)} - G_4^{(in)}G_5^{(in)}\right)}{\left(G_7^{(in)}\right)^3}\Phi'(\det(\Sigma_{in})) \\ A_7^{(in)} = \displaystyle\int\int_{\Omega_{in}(\tau)} \frac{\partial g}{\partial G_7^{(in)}} = \int\int_{\Omega_{in}(\tau)} \frac{-3Z^{(in)}}{\left(G_7^{(in)}\right)^4}\Phi'(\det(\Sigma_{in})) \end{cases}$$

And by expressing the covariance matrix with the functions $G_j^{(in)}$ as following:

$$\Sigma_{in} = \begin{pmatrix} \frac{G_1^{(in)}}{G_7^{(in)}} & \frac{G_4^{(in)}}{G_7^{(in)}} & \frac{G_5^{(in)}}{G_7^{(in)}} \\ \frac{G_4^{(in)}}{G_7^{(in)}} & \frac{G_2^{(in)}}{G_7^{(in)}} & \frac{G_6^{(in)}}{G_7^{(in)}} \\ \frac{G_5^{(in)}}{G_7^{(in)}} & \frac{G_6^{(in)}}{G_7^{(in)}} & \frac{G_3^{(in)}}{G_7^{(in)}} \end{pmatrix}$$

We then deduce:

$$\begin{cases} A_1^{(in)} = (-1)^{(1+1)}\det\left(M_{in}^{11}\right)\Phi'(\det(\Sigma_{in})) \\ A_2^{(in)} = (-1)^{(2+2)}\det\left(M_{in}^{22}\right)\Phi'(\det(\Sigma_{in})) \\ A_3^{(in)} = (-1)^{(3+3)}\det\left(M_{in}^{33}\right)\Phi'(\det(\Sigma_{in})) \\ A_4^{(in)} = (-1)^{(1+2)}2\det\left(M_{in}^{12}\right)\Phi'(\det(\Sigma_{in})) \\ A_5^{(in)} = (-1)^{(1+3)}2\det\left(M_{in}^{13}\right)\Phi'(\det(\Sigma_{in})) \\ A_6^{(in)} = (-1)^{(2+3)}2\det\left(M_{in}^{23}\right)\Phi'(\det(\Sigma_{in})) \\ A_7^{(in)} = -3\det(\Sigma_{in})\Phi'(\det(\Sigma_{in})) \end{cases}$$

where M_{in}^{kl} is the matrix deduced from Σ_{in} by suppressing the kth row and the lth column. The computation for the descriptor $k^{(out)}$ is similar and we then have all the expressions to compute the evolution equation from the general formula (14). This gives the evolution equation.

References

Amadieu, O., Debreuve, E., Barlaud, M., and Aubert, G. 1999. Inward and outward curve evolution using level set method. In *International Conference on Image Processing*. Kobe, Japan.

Amonou, I. and Duhamel, P. 2000. Iterative backward segmentation for hierarchical wavelet image coding. In *International Conference on Image Processing*. Vancouver, Canada.

Aubert, G., Barlaud, M., Faugeras, O., and Jehan-Besson, S. Image segmentation using active contours: Calculous of variation or shape optimization? To appear in SIAM Applied Mathematics.

Aubert, G. and Kornprobst, P. 2001. Mathematical problems in image processing. Partial differential equations and the calculus of variations, No. 147. Applied Mathematical Sciences, Springer Verlag.

Caselles, V., Catte, F., Coll, T., and Dibos, F. 1993. A geometric model for active contours in image processing. In *Numerische Mathematik*, vol. 66, pp. 1–33.

Caselles, V., Kimmel, R., and Sapiro, G. 1997. Geodesic active contours. *International Journal of Computer Vision*, 22(1):61–79.

Chakraborty, A. and Duncan, J. 1999. Game-theoretic integration for image segmentation. *IEEE Transactions on Pattern Analysis and Machine Intelligence*.

Chakraborty, A., Staib, L., and Duncan, J. 1996. Deformable boundary finding in medical images by integrating gradient and region information. *IEEE Transactions on Medical Imaging*, 15:859–870.

Chan, T. and Vese, L. 2001. Active contours without edges. *IEEE Transactions on Image Processing*, 10(2):266–277.

Chesnaud, C., Réfrégier, P., and Boulet, V. 1999. Statistical region snake-based segmentation adapted to different physical noise models. *IEEE Transactions on Pattern Analysis and Machine Intelligence*, 21:1145–1156.

Cohen, L. 1991. On active contour models and balloons. *Computer Vision, Graphics and Image Processing: Image Understanding*, 53:211–218.

Cohen, L., Bardinet, E., and Ayache, N. 1993. Surface reconstruction using active contour models. In *SPIE Conference on Geometric Methods in Computer Vision*. San Diego, CA.

Debreuve, E. 2000. Segmentation par contours actifs en imagerie médicale dynamique: Application en cardiologie nucléaire. Ph.D. thesis, University of Nice-Sophia Antipolis, France.

Debreuve, E., Barlaud, M., Aubert, G., and Darcourt, J. 2001. Space time segmentation using level set active contours applied to myocardial gated SPECT. *IEEE Transactions on Medical Imaging*, 20(7):643–659.

Delfour, M. and Zolésio, J.-P. 2001. *Shapes and Geometries*, Advances in Design and Control, Siam.

Delingette, H. and Montagnat, J. 2001. Topology and shape constraints on parametric active contours. *Computer Vision and Image Understanding*, 83(2):140–171.

Goldenberg, R., Kimmel, R., Rivlin, E., and Rudzsky, M. 2001. Fast geodesic active contours. In *IEEE Transactions on Image Processing*, vol. 10, pp. 1467–1475.

Gomes, J. and Faugeras, O. 2000. Reconciling distance functions and level sets. *Journal of Visual Communication and Image Representation*, 11:209–223.

Gray, R. and Davidson, L. 2000. *An Introduction to Statistical Signal Processing*. Version libre.

Gray, R., Young, J., and Aiyer, A. 2001. Minimum discrimination information clustering: Modeling and quantization with gauss mixtures. In *International Conference on Image Processing*. Thessaloniki, Greece.

Jehan-Besson, S., Barlaud, M., and Aubert, G. 2000. Detection and tracking of moving objects using a new level set based method. In *International Conference on Pattern Recognition*, Barcelona, Spain, vol. 3, pp. 1112–1117.

Jehan-Besson, S., Barlaud, M., and Aubert, G. 2001a. Region-based active contours for video object segmentation with camera compensation. In *International Conference on Image Processing*. Thessaloniki, Greece.

Jehan-Besson, S., Barlaud, M., and Aubert, G. 2001b. Video object segmentation using eulerian region-based active contours. In *International Conference on Computer Vision*. Vancouver, Canada.

Jehan-Besson, S., Barlaud, M., and Aubert, G. 2002. A 3-Step algorithm using region-based active contours for video objects detection. *EURASIP Journal on Applied Signal Processing. Special Issue on Image Analysis for Multimedia Interactive Services*, 2002(6):572–581.

Kass, M., Witkin, A., and Terzopoulos, D. 1988. Snakes: Active contour models. *International Journal of Computer Vision*, 1:321–332.

Malladi, R., Sethian, J., and Vemuri, B. 1995. Shape modeling with front propagation: A level set approach. *IEEE Transactions on Pattern Analysis and Machine Intelligence*, 17:158–175.

Mansouri, A. and Konrad, J. 1999. Motion segmentation with level sets. In *International Conference on Image Processing*. Kobe, Japan.

Montagnat, J., Delingette, H., and Ayache, N. 2001. A review of deformable surfaces: Topology, geometry and deformation. *Image and Vision Computing*, 19(14):1023–1040.

MPEG-7. 1998. MPEG-7 Context and Objectives. Technical report, International Organization for Standardization, ISO/IEC JTC1/SC29/WG11 N2460.

MPEG-7. 2000. Requirements document (V12). Technical report, International Organization for Standardization, ISO/IEC JTC1/SC29/WG11 W3548.

Mumford, D. and Shah, J. 1989. Optimal approximations by piecewise smooth functions and associated variational problems. *Communications on Pure and Applied Mathematics*, 42:577–684.

Osher, S. and Sethian, J. 1988. Fronts propagating with curvature-dependent speed: Algorithms based on Hamilton-Jacobi Formulation. *Journal of Computational Physics*, 79:12–49.

Paragios, N. and Deriche, R. 1999a. Geodesic active regions for motion estimation and tracking. In *International Conference on Computer Vision*. Corfu Greece.

Paragios, N. and Deriche, R. 1999b. Geodesic active regions for motion estimation and tracking. In *International Conference on Computer Vision*. Corfu Greece.

Paragios, N. and Deriche, R. 2000. Coupled Geodesic Active Regions for Image Segmentation: A Level Set Approach. In *European Conference in Computer Vision*. Dublin, Ireland.

Paragios, N. and Deriche, R. 2002a. Geodesic Active Regions: A new Paradigm to deal with frame partition Problems in Computer vision. *Journal of Visual Communication and Image Representation*, 13:249–268.

Paragios, N. and Deriche, R. 2002b. Geodesic active regions and level set methods for supervised texture segmentation. *International Journal of Computer Vision*, 46(3):223.

Pateux, S. 2000. Spatial segmentation of color images according to MDL formalism. In *International Conference on Color in Graphics and Image Processing*. Saint Étienne, France.

Precioso, F. and Barlaud, M. 2001. B-Spline active contours for fast video segmentation. In *International Conference on Image Processing*. Thessaloniki, Greece.

Ronfard, R. 1994. Region-based strategies for active contour models. *International Journal of Computer Vision*, 13(2):229–251.

Salembier, P. 1994. Morphological multiscale segmentation for image coding. *Signal Processing*, 38:359–386.

Samson, C., Blanc-Féraud, L., Aubert, G., and Zerubia, J. 2000. A level set model for image classification. *International Journal of Computer Vision*, 40(3):187–197.

Schnörr, C. 1992. Computation of discontinuous optical flow by domain decomposition and shape optimization. *IJCV*, 8(2):153–165.

Sethian, J. 1990. Numerical algorithms for propagating interfaces: Hamilton-Jacobi equations and conservation laws. *Journal of Differential Geometry*, 31:131–161.

Sethian, J. 1996. *Level Set Methods*. Cambridge Univ. Press.

Siddiqi, K., Lauzière, Y., Tannenbaum, A., and Zucker, S. 1996. Area and length minimizing flows for shape segmentation. *IEEE Transactions on Image Processing*, 7(3):433–443.

Sokolowski, J. and Zolésio, J.-P. 1992. Introduction to shape optimization. Shape sensitivity analysis. Vol. 16 of *Springer Ser. Comput. Math*. Springer-Verlag, Berlin.

Weickert, J., Haar Romeny, B., and Viergerer, M.A. 1998. Efficient and reliable scheme for nonlinear diffusion filtering. *IEEE Transaction on Image Processing*, 7(3):398–410.

Yezzi, A., Tsai, A., and Willsky, A. 1999. A statistical approach to snakes for bimodal and trimodal imagery. In *International Conference on Image Processing*. Kobe, Japan.

Zhu, S., Lee, T., and Yuille, A. 1995. Region competition: Unifying snakes, region growing, and Bayes/MDL for multiband image segmentation. In *International Conference on Computer Vision*, pp. 416–423.

Zhu, S. and Yuille, A. 1996a. Region competition: Unifying snakes, region growing, and Bayes/MDL for multiband image segmentation. *IEEE Transactions on Pattern Analysis and Machine Intelligence*, 18:884–900.

Zhu, S. and Yuille, A. 1996b. Region competition: Unifying snakes, region growing, and Bayes/MDL for multiband image segmentation. *IEEE Transactions on Pattern Analysis and Machine Intelligence*, 18:884–900.